2000

Transient stability assessment and decision-making using risk

Vincent Eric A. Van Acker
Iowa State University

INFORMATION TO USERS

This manuscript has been reproduced from the microfilm master. UMI films the text directly from the original or copy submitted. Thus, some thesis and dissertation copies are in typewriter face, while others may be from any type of computer printer.

The quality of this reproduction is dependent upon the quality of the copy submitted. Broken or indistinct print, colored or poor quality illustrations and photographs, print bleedthrough, substandard margins, and improper alignment can adversely affect reproduction.

In the unlikely event that the author did not send UMI a complete manuscript and there are missing pages, these will be noted. Also, if unauthorized copyright material had to be removed, a note will indicate the deletion.

Oversize materials (e.g., maps, drawings, charts) are reproduced by sectioning the original, beginning at the upper left-hand corner and continuing from left to right in equal sections with small overlaps.

Photographs included in the original manuscript have been reproduced xerographically in this copy. Higher quality 6" x 9" black and white photographic prints are available for any photographs or illustrations appearing in this copy for an additional charge. Contact UMI directly to order.

Bell & Howell Information and Learning
300 North Zeeb Road, Ann Arbor, MI 48106-1346 USA
800-521-0600

Transient stability assessment and decision-making using risk

by

Vincent Eric A. Van Acker

A dissertation submitted to the graduate faculty
in partial fulfillment of the requirements for the degree of
DOCTOR OF PHILOSOPHY

Major: Electrical Engineering (Electric Power)
Major Professor: James D. McCalley

Iowa State University
Ames, Iowa
2000

Bell & Howell Information and Learning Company
300 North Zeeb Road
P.O. Box 1346
Ann Arbor, MI 48106-1346

Graduate College

Iowa State University

This is to certify that the Doctoral dissertation of

Vincent Eric A. Van Acker

has met the dissertation requirements of Iowa State University

Signature was redacted for privacy.

Major Professor

Signature was redacted for privacy.

For the Major Program

Signature was redacted for privacy.

For the Graduate College

"The only way to discover the limits of the possible is to go beyond them into the impossible."

Arthur C. Clarke

TABLE OF CONTENTS

1. INTRODUCTION

For many decades, electric power systems have been operated within the boundaries of operating limits imposed by safe but conservative reliability criteria. This approach has served the industry very well over many years, providing energy at high reliability levels. Nowadays, with the current changes in the electric power market towards deregulation, the operators are more and more pressured to operate very close to the operating limits, and thus with smaller security margins. Therefore, it is crucial for them to know exactly what these limits are.

Power system deregulation has also forced the operators to integrate some economic awareness in their decision making when monitoring the system. It is no longer sufficient just to know that the system is being operated at the traditionally safe side of the operating limits; they also want to know what the economic consequences are of operating at a certain point considering more than just the most limiting disturbances. In other words, the operators want to know what the *risk* is that they are incurring over a certain period of time while operating at a specific operating point. This information will allow them to make much 'better' decisions in the sense that the decisions will be more defendable because they are based on more relevant information.

1.1 Deterministic operating limits

Power systems cannot be made completely safe even with infinite expenditure. That is why a set of limits is used to maintain a reasonable level of reliability. Traditionally, these limits are defined based on disturbance-performance criteria [1][2] and are identified as follows: using a chosen system configuration, a list of vital components is set up. Each one of

these components is removed and the system is assessed for thermal overload, transient and voltage security under a selected set of operating conditions. In what follows, the event of losing one or more components will be referred to as a *contingency*. By repeatedly simulating different conditions, an operating region is identified, where the system performance following the contingency satisfies the disturbance-performance criteria. Next, the component is put back in service and the next component in the list is removed from the system and the process is repeated. At the end, the intersection of all safe areas is taken as the acceptable security region (Figure 1-1).

As can be seen from Figure 1-1, out of a huge list of contingencies, actually only a few will define the edges of the security region. The two-dimensional diagram presented below, also called nomograms, is used by many utilities to assess the security of their system by locating the current operating state in this diagram and by avoiding the insecure region. Nomograms are usually plotted in the space of two critical operating parameters.

The motivation behind the use of this deterministic approach is that it shields the system from fault related uncertainties. A few very severe but not necessarily likely disturbances are considered, and the system is operated in such a way that it can perform well

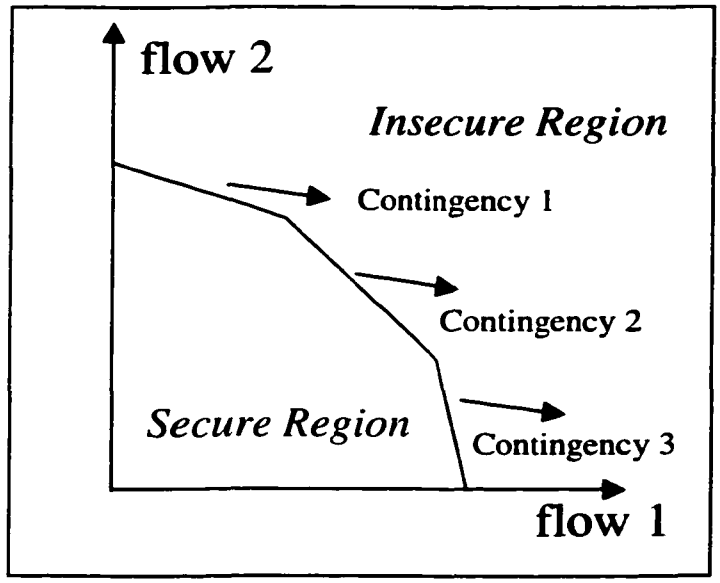

Figure 1-1. Deterministic security region

even if these disturbances occur. Typically the contingencies considered consist of all single component outages, considering there are "N" components, this is called the "N-1" contingency selection criteria.

With the current trend towards competitive and deregulated electricity market environment, the utilities are forced to guarantee, besides a safe reliability level, also an economical operational efficiency. They are feeling some pressure to maximize the utilization of their existing facilities and are facing tough environmental restrictions building new transmission lines. As a consequence, some operators may consider exploring the operating areas beyond the traditional operating limits, where the system is vulnerable to costly outages, in order to see if the incurred risk weighs against the potential economic benefits of violating the limits. In these circumstances a risk assessment tool becomes also extremely useful.

It would be very helpful to identify the level of accumulated danger induced by all contingencies, considering their probability of occurrence and their consequences should they occur, within the traditionally safe region as well as outside of it. A 'danger' or 'risk' index would help the system operator to discover operating areas where the probabilities of insecurity events or the impact of these events is low. Such an index is defined in this work and is called risk. It combines both the probability of the insecurity events and the consequences of these events, should they occur. A method is developed to quantify the measure of risk. The risk index includes impact and likelihood information of a large list of credible contingencies, as opposed to the N-1 deterministic limit approach where only the worst-case scenario was considered.

Several authors have considered both the probability and impact of disturbances: Silverstein and Porter [3] provided a disturbance-performance table for planning where lower performance levels are acceptable for events that are less likely to occur. Alvarado et al. [4] used the idea of security regions to develop an expected outage cost for voltage instability. Leite da Silva et al., [5] developed a framework for integrating adequacy and security assessment, resulting in computation of probabilistic indices for pre-disturbance conditions. Counan, et al. [6] devised a defense plan against extremely low probability but very severe

system collapse mechanisms. More recently, Aboreshaid et al. [7] define well-being states and the probability that the system is residing in each state is calculated.

Each one of these works comes short of defining an index that measures the risk to which the system is exposed at the current operating conditions. In a planning environment, reliability indices are used such as is the *loss of load probability* (LOLP), which only includes a reference to the probability but not the impact. Other indices like *expected unserved energy* (EUE) and the *loss of load expectation* (LOLE) do include some measure of severity, but they are restricted to loss of load (customer interruption) and do not account for equipment damage or costs due to equipment unavailibilty. For example, Porretta, et al. [8] developed a risk-based index that is appropriate for use in a planning environment but here again, the only impact that is considered is the load interruption.

1.2 Risk-based security assessment

In this work, risk can be more formally defined as the expected cost consequences of an insecurity event K over a period of time depending on fault parameters p, at a given vector of operating conditions $\bar{x}$. It can be computed as follows:

$$Risk(K(p) \mid \bar{x}) = \int \Pr(K(p) \mid \bar{x}) \cdot \mathrm{Im}(K(p) \mid \bar{x}) \cdot dp \qquad (1\text{-}1)$$

Insecurity events K can be for example, transmission circuit or transformer overload, voltage or transient instability. Risk-based security assessment using the above definition of risk has been discussed in reference [9]. In reference [10] Wan developed a method to assess the risk of thermal overload of a circuit and showed how the thermal ratings of the lines can be increased if the thermal overload is approached from a risk point of view. In [11] the same author also defined risk-based voltage instability. While the risk assessment discussed in this dissertation is focused on an operation environment, in reference [12] Dai presented a framework for power system risk assessment in the planning by defining annual risk, accumulated from an expected system trajectory. In reference [13], Fu addressed different

risk-related topics: impact assessment for risk-based security assessment, risk assessment for transformer overload, risk assessment for special protection systems, risk assessment for bilateral transactions, and risk-based optimal power flow.

The major part of this research is dedicated to the development of a methodology to evaluate risk of a distinct insecurity problem, namely, the transient instability. Some specific features of this type of risk assessment, as well as ways to alleviate the computationally intensive procedure, are discussed. In addition, a risk-based decision-making framework is presented, capable of assisting the system operator to deal with conflicting decision criteria in an operation environment.

1.3 Deterministic limits are risk inconsistent

Previously in this chapter it was mentioned that many utilities are using the (deterministic) nomograms to control the security of the system in an operating environment. The definition of risk permits evaluating the level of risk at any point in this diagram, within the traditionally safe region and outside of it. The measure of risk will allow to estimate how dangerous it really is to cross these deterministic limits.

The deterministic limits are imposed by different contingencies. The contingencies have a different probability of occurrence, and when they occur they also have a different impact. As a result, they correspond to different levels of risk. If the contours of equal risk would be drawn on the nomogram of Figure 1-1, the resulting risk-based nomogram could look something like Figure 1-2. The bold curved line connects lines with equal value of risk and clearly reveals the inconsistencies in terms of incurred risk inherent to the deterministic operating limits; some operating points in the safe region actually have a higher risk value than some points in the insecure region. This diagram would permit the operators to choose the risk level they judge appropriate for their system and could use the corresponding risk contour as the new operating limit.

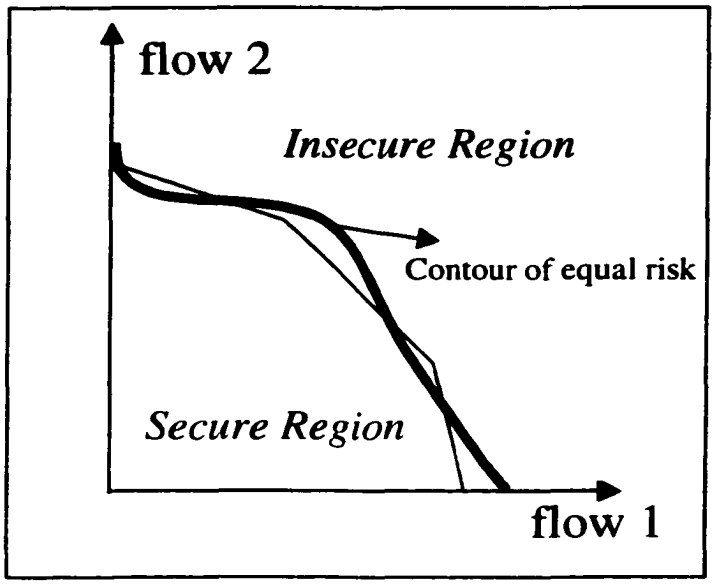

Figure 1-2. Risk-based nomograms.

1.4 Risk-based decision-making

The previous section already pointed out the type of decision operators may face: which level of risk is appropriate for their system. With the increased urge to operate close or even beyond the traditional operating limits, on many occasions the system operators face the sometimes-critical situation where they have to decide among several operating options, some of them being risky. For example, they may face the situation where they need to decide between shedding load, buying power from neighboring area, changing the system configuration or not changing anything at all. Their decision will affect the lives of thousands, even millions of people, as well as the future of their jobs in particular.

Risk is an excellent tool to assist the system operators to make the most appropriate (or most defendable) decision, as it will permit them to weigh the possible adverse consequences of the options against their benefits. One of the aims of this research is to show how risk can be used to assist the operator in making crucial decisions regarding the operation of the system.

1.5 Contribution of this work

In this dissertation, a further development of the Risk Based Security Assessment (RBSA) is presented, with special emphasis on the risk of transient instability; it focuses on an index describing the instability risk for generators individually. To be useable in an operation environment, the calculation time should be reasonable and various ways to alleviate the calculation procedure, in particular the use of artificial neural networks are presented.

In addition, a risk management method is developed by proposing a multi-criteria decision-making framework based on risk. It enables the operator to balance the economic operation aspects and security considerations in order to make informed and defendable decisions in a short amount of time.

1.6 Organization of the document

In Chapter 2, the existing transient stability assessment techniques are discussed, with special emphasis on the hybrid methods. One such method is explained in more detail as it has the features required for risk calculations. Chapter 3 is dedicated to risk of transient instability: the probabilistic modeling of the relevant uncertainties is discussed and the expressions to calculate the risk of transient instability are derived. Next, in chapter 4, the influence of different parameters on the risk of transient instability is observed by applying the methodology presented in chapter 3 to the IEEE test system. Chapter 5 deals with one of the major problems of the proposed risk procedure, namely the heavy computational effort required. Finally, having defined a way to evaluate the risk of transient instability for a given operating point, Chapter 6 shows how this index can be conveniently used in an operational decision making framework. Chapter 7 closes this dissertation with some concluding remarks and some suggestions for future work.

2. TRANSIENT STABILITY ASSESSMENT

Stability is a very broad concept. When talking about stability of a power system it is referred to as the ability of the system to regain an acceptable equilibrium state after a disturbance or to maintain acceptable equilibrium state under normal operating conditions. Many different types of stability exist [14].

Table 2-1. Different types of instability

Instability	***Description***
Transient	Synchronous machine rotor angle separation after severe disturbance
Small Signal	Inability to remain stable under small disturbances
Oscillatory	Insufficient damping torque to decrease the oscillations amplitude
Voltage	Voltage collapse due to insufficient reactive support

This work focuses on transient stability. Transient stability analysis considers the performance of a power system subjected to a severe disturbance such as a shunt fault, tripping of a phase or an interconnection, loss of a large generator, or a sudden increase in load. System stability behavior is directly related with the transient behavior of the synchronous machines present in a power system following such a disturbance. Under severe circumstances, one or more generators may not be able to remain in synchronism with the rest of the system and will go unstable. The rotor angle of the unstable machines will separate from those of the other units. This is also referred to as a generator out-of-step condition. The generator will be disconnected from the grid due to the operation of the protection relays or part of the system will be isolated (islanding) from the rest of the system in order to prevent the remaining part to collapse.

The more power the generator is supplying, the likelier it is that it will go out-of-step, because the power unbalance resulting from the fault will be larger. In addition, the severity of disturbance caused by the fault tends to increase as the fault moves closer to the generator bus.

This chapter offers a brief discussion of the different transient stability assessment methods. One particular method will be explained in more detail as it is employed in the risk calculations in the following chapters.

2.1 Transient stability assessment techniques

2.1.1 Numerical integration of differential equations

When setting up the mathematical model of a power system with its components, the most conventional way to observe its dynamic behavior after a disturbance is by numerically integrating a set of differential equations over a certain period. This technique is also called assessment by *time domain simulation*. Since virtually any component can be included in this mathematical model, there are no modeling limitations.

Many books in the literature focus on the modeling of the different elements in the system as well as on the numerical techniques available to perform the time domain simulation [15][16]. The methods differ in accuracy, numerical stability and speed. Some of the most commonly used numerical integration methods are the Euler method, and the 2^{nd} and 4^{th} order Runge-Kutta method. Other more sophisticated methods have also been used, like the Adams-Bashfort predictor formula and the Adams-Moulton correctors formula. The solving process with these methods is considerably faster and numerically robust [17].

The weaknesses of these methods lie in the enormous computational effort required, especially for real-sized networks with a large number of disturbances to analyze. Despite the progress of the present day computer technology, this method is still too slow to be used in an operation environment. On the other hand, in a planning environment, where time is not such a factor, time domain simulations can be very useful because they produce very accurate time plots of all possible parameters.

Another weakness of the time domain simulation methods is that a system is declared stable or unstable after observing (visually or numerically) the time responses of the relative rotor angles; there is no clear quantitative indicator to tell that the system is stable or not such that the simulation can be interrupted. This is an obstacle that makes automating a large sequence of assessments very difficult.

Finally, when performing the time domain simulation the only possible outcome is an answer to the question whether the system is stable or not. It does not produce any type of stability measure. It is not easy to tell whether an unstable case is clearly or just marginally unstable.

2.1.2 Direct methods

Following the blackout in the USA in 1965, a lot of effort was spent in research to develop tools that would make on-line transient stability assessment possible. Researchers have tried to develop a method that returns directly the degree of stability of a faulted power system based on the Lyapunov theory [18],[19]. An energy function is defined which can be used to give a stability measure of the system. The energy injected in the system during the fault can be calculated and compared to the critical energy of the system under that fault. If the injected energy is larger than this critical value, the system will go unstable – at least one machine loses synchronism with the rest of the machines. On the other hand, if the injected energy is smaller than the critical energy, the system will remain stable. The Transient Energy Function methods, called direct methods, are known to be very fast compared to traditional time domain simulation, and they provide the desired stability measure.

The early versions of the method were considered largely conservative. However, with the contributions at the end of the 70's, the credibility of the direct methods increased. The concept of potential energy boundary surface (PEBS) was introduced by Kakimoto et al. [20]. Methods to determine the relevant or controlling unstable equilibrium point (CUEP) were presented in reference [21] and improved with the boundary of stability-region-based CUEP method proposed by Chiang et al. [22]. However, despite some significant progress made in the last decade the modeling capabilities have always been somewhat limited. In

addition, unreliability of the numerical techniques used has resulted in a certain reluctance to use them widely.

In the late 80's, Xue et al. ([23],[24]) developed a somewhat different direct method, where the equal area criterion is used for multi-machine power systems, and they called it *extended equal area criterion* (EEAC). It consists in transforming the multimachine power system into two equivalent machine systems. The two-machine dynamic equivalent is then further reduced to a one-machine-infinite-bus (OMIB) system. The critical clearing time can now be calculated using the equal area criterion applied to the OMIB.

2.1.3 Hybrid methods

In the past decade, many authors have attempted to incorporate transient energy analysis into the time domain simulation. It is believed that this way the best compromise is obtained between speed and accuracy when combining the good features of both direct methods and time domain simulation. These methods are commonly referred to as the 'hybrid methods'. Fouad et al. [25] derived a quantitative stability index for each machine in the system from the time domain simulation program output analysis. In [26], Maria et al. use the Energy Function of the entire system and the output results of the time domain simulation to find a stability margin or index. Line searches along linear angle paths are required to find the crossing point with the potential energy surfaces associated with classical machine representation. Tang et al. in [27] present a variation of the method, called the 'second kick method', removing the classical model restriction in detecting the PEBS and by replacing the line search with a pseudo-fault-on trajectory. Other combinations of methods appeared, e.g., combining equal area criterion with the PEBS method. Zhang et al.[29] propose a method called SIME (SIngle Machine Infinite bus Equivalent) that combines the above mentioned EEAC-method with time domain simulation. At each iteration, the two-machine equivalent is recalculated, followed by the single machine equivalent, using the output of the time domain simulation. Other combinations exist; in reference [28] EEAC-method is used together with the PEBS-concept.

2.1.4 Transient stability index method (TSI-method)

As will be shown later in this work, the speed is a very important factor in the risk calculation. If time domain simulations were to be used as the transient stability assessment technique, the risk calculation procedure would be far too time-consuming to be used in an operation environment, let alone on-line. In the previous section it was stated that the hybrid methods perform well both in terms of accuracy and speed. That is why in this work a hybrid method is applied.

In Reference [30], Ejebe et al. propose a method using time domain simulation to calculate energy components at each iteration. An early termination criterion is used to stop the simulation when the stability or instability has been confirmed and at that point a transient stability index is obtained. To alleviate the notations and expressions, from this point on this index will be named φ.

The TSI method is computationally simple and φ is very easy to obtain. The method is also very intuitive because the index is closely related with the transient behavior of the system. In addition, contrary to other hybrid methods, to calculate the stability index, only the results of the post-fault trajectory are used; there is no need for a re-insertion of an artificial fault after the fault clearing as there is using the 'second kick' method. However, this method only detects first-swing stability.

The method consists in monitoring the sign of two dot products associated to transient energy components: accelerating power/angle or *ftheta* (Eq. 2-1) and speed/angle or *speedtheta* (Eq. 2-2).

$$f(\theta)\cdot(\theta-\theta_s) \tag{2-1}$$

$$\tilde{\omega}\cdot(\theta-\theta_s) \tag{2-2}$$

where f is the vector of accelerating powers, θ is the vector of angles referred to the center of inertia and θ_s is the vector of angles at the post-fault stable equilibrium point (sep). $\tilde{\omega}$ represents the speed vector referred to the center of inertia.

After the fault is cleared, the simulation will go on until a change of sign occurs in any of the two dot products. A change of sign in the first dot product (Eq. 2-1) before the second dot product (Eq. 2-2) indicates that the system trajectory crosses the PEBS, revealing

an *unstable* situation. Not all the kinetic energy has been absorbed by the post-fault system. The moment at which this change of sign occurs is recorded as the exit time t_{exit} (Figure 2-1).

On the other hand, if the second dot product changes sign before the first one, the system trajectory starts to swing back and is therefore *stable*. The system will eventually progress to the original stable equilibrium point, or to a new one if switching has occurred while clearing. The moment at which this change of sign occurs is recorded as the swing back time $t_{swingback}$ (Figure 2-2).

It can best be explained by using the analogy of a car that is given a push towards an up-hill slope: the push is representing the fault, and the car will climb the hill while it loses speed. If the push is strong, it will roll over the top, and start rolling down the hill at the other

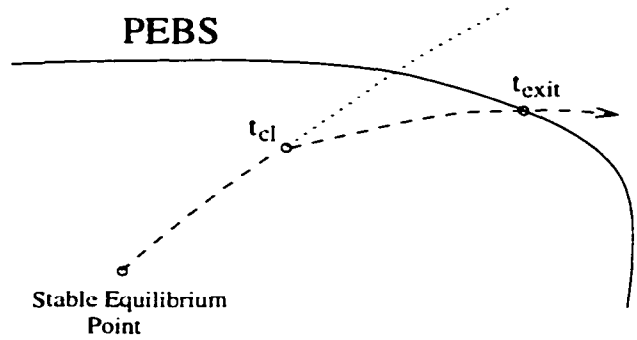

Figure 2-1. Trajectory of unstable case.

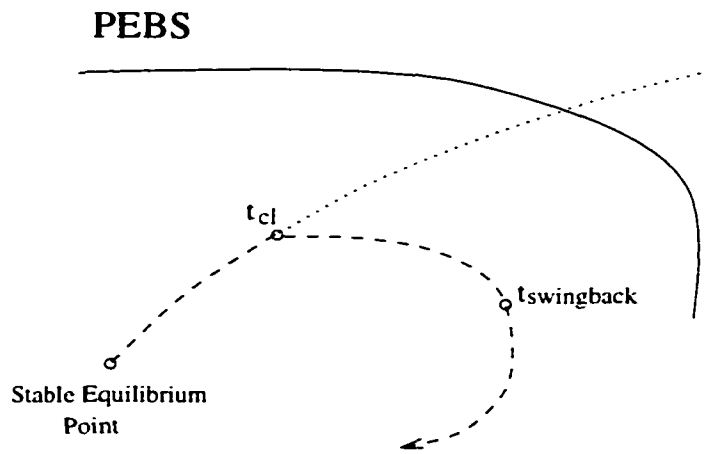

Figure 2-2. Trajectory of stable case.

side and will accelerate. The kinetic energy could not all be absorbed while climbing the slope. The accelerating power changes sign, and therefore also *ftheta*. In the other situation where the car does not reaches the top but starts rolling down backwards somewhere on the slope, *speedtheta* will change sign; it means that the push was not so strong, and that the kinetic energy has already been absorbed before the car reaches the top. After a change of sign occurs, the simulation is stopped: this early termination criterion limits the time domain simulation time to a maximum of 2 or 3 seconds. The index φ is defined as follows:

$$\varphi = \begin{cases} \dfrac{1}{t_{sb}} & \text{if stable} \\ -\dfrac{1}{t_{exit}} & \text{if unstable} \end{cases} \qquad (2\text{-}3)$$

The complete algorithm for the calculation if φ is depicted in Figure 2-3.

When a very unstable case is simulated, the trajectory will quickly reach the PEBS, so that the exit time will be very small, and subsequently, the φ very negative. Analogously, a very stable situation will result in a large positive φ, because it will swing back quickly.

In Figure 2-4, an example is given of the influence of two fault parameters on the index φ: For each fault type, the index is plotted against the distance of the fault from the generator bus. It can be seen that for this particular situation the generator remains stable for any single-phase fault, and the generator goes out-of-step for any three-phase faults closer than 80% of the total line length.

For the purpose of this work, the TSI-method was considered appropriate and is conveniently used in the probability calculations, as will be explained later. Nevertheless, any other method that is fast and that returns a numerical measure of stability could have been applied.

In the next chapter, it will be explained how this index is used in the risk calculation procedure.

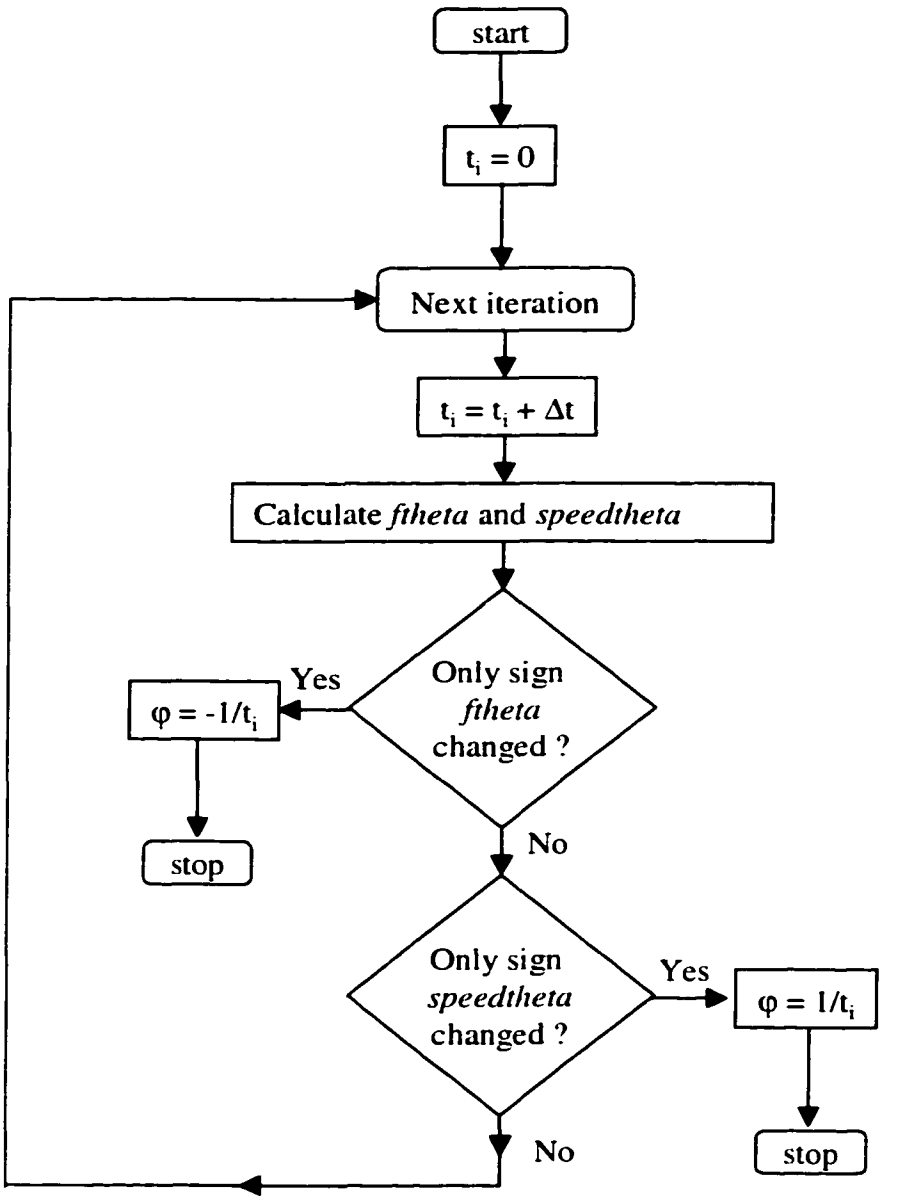

Figure 2-3. Calculation procedure for the transient stability index φ

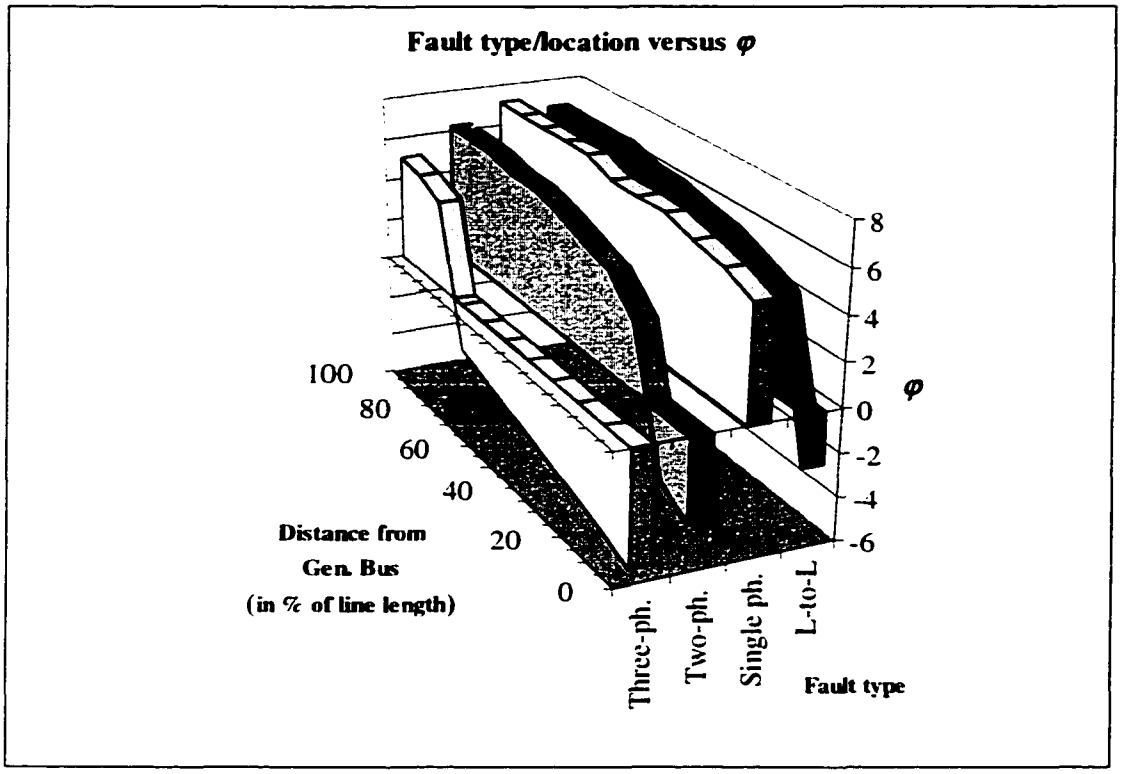

Figure 2-4. Influence of location and fault type on the φ index

2.2 Summary of chapter

This chapter focuses mainly on transient stability and the different stability assessment techniques. The two categories of methods are described and their weaknesses are discussed. A third category of methods is presented, the hybrid methods, combining the good features of different transient stability assessment techniques. The hybrid method used in this work, the TSI-method, is explained in more detail.

3. RISK-BASED TRANSIENT INSTABILITY

In many power systems the operator is concerned about the stability behavior of one particular plant that may go unstable for certain faults and under certain operating conditions. Traditionally, imposing deterministic security limits certify the security of that plant. These limits are defined as the maximum generator or plant power output where a three-phase fault at the generator bus would still not lead to instability, eventually with some safety margin. As mentioned earlier, the worst-case credible scenario is thought to safeguard the system against the uncertainties associated with the consequences of a fault occurrence and with fluctuations of pre-fault conditions over the study period. It is very difficult to get an accurate measurement of the probabilities of, for example, cascading events. Instead of going through this complex calculation, the deterministic method simply adopts a conservative rule, accounting for a large number of uncertainties.

An example of how conservative these criteria can be is illustrated in Table 3-1 below. The system on which these numbers were taken is presented in section 4.1. The results presented further in this chapter, and later chapters are obtained using the same system. The plant at Bus 13 consists of three identical 200MW generators that are at risk of going unstable, for faults on either line 12-13 or 13-23. Line 11-13 is assumed to be out of service for scheduled maintenance.

The table contains the maximum safe generation levels under each fault type and at each line end on either one of the two lines leaving from the generator bus. It can be seen that keeping the generation levels below the deterministic limit associated with a three phase at the generator terminals (460 MW) the plant is underused, since it has a capability of producing 600 MW.[1]

[1] When the security limit is higher than the maximum 600 MW capacity limit, the values are indicated in gray.

Table 3-1. Power limit levels (MW) for different fault types and locations.

Line	*Location*	*Three phase*	*Two phase*	*Line-to-line*	*Single phase*
Line 1	Near end	460	490	516	564
	Far end	534	600	600	600
Line 2	Near end	460	486	513	560
	Far end	561	594	600	600

From historical data it is observed that the majority of faults do not occur at the generator terminals and the most severe type of fault, the three-phase fault, has a very low probability. Moreover, the factors conditioning the disturbances, such as the fault characteristics and the pre-fault operating state are probabilistic in nature, and therefore it seems natural to examine them from that point of view.

In short, the drawback of the deterministic approach is that it results in quite expensive operating conditions, and excellent sales opportunities at low risk can be lost because of these severe requirements.

The risk-based approach proposed in this work has a similar structure as other security problems that have been addressed in earlier works (see chapter 1). In the next section, an overview is presented of the relevant work regarding probabilistic assessment of transient instability.

3.1 Review of previous work

A considerable amount of literature is available on probabilistic transient stability assessment. In the late 70's Burchet et al. [31] evaluated dynamic stability by considering the stochastic nature of power system parameters. A few years later, a series of papers by Billinton and Kuruganty [32]-[34] were published presenting an analytical approach to determining the probability of transient stability by evaluating the probability distribution for the critical clearing time, fault location and fault type and a probability index was defined. They also discuss a way to model the protection system probabilistically [35]. Anderson,

Bose, and colleagues [36]-[38] proposed computing a stability distribution from probabilistic representation of the event space: disturbance location, type, and sequence. They employed Monte-Carlo simulation in this computation. Wu et al. [39] proposed an approach based on measuring the time to insecurity. In [41] and [42] the probabilistic nature of the pre-fault conditions are taken into account to calculate the conditional probability of instability. In a more recent publication from Momoh et al., a probabilistic assessment is presented using a measure for the expected angle stability margin [43].

Besides probability, risk also includes at the consequences of the system performance when the instability has occurred. Dodu and Merlin [44] used Monte-Carlo simulation to estimate expected energy not served due to transient instability.

The first attempt toward risk-based transient stability was presented by Irizarry-Rivera in [45] and [46], where the concept of limiting operating point functions is employed. These functions return the limiting generation level for any fault type and fault location on a certain circuit. This work has been extended in this dissertation.

3.2 Chapter overview

In real operating circumstances, the potential transient instability problems that may occur in a network are often local and well identified. In this case, the operators usually know which generator has a tendency of going *out-of-step* depending on the operating conditions. That is why for them, an index evaluating the risk of this local trouble spot is more helpful than a global stability index. In the work described in this chapter, an approach is presented that calculates risk of transient instability of a particular plant, by using clarified probability expressions, including a more extensive uncertainty modeling, and the impact assessment looks at several possible consequences caused by the instability event and quantifies this in monetary units. The probability of transient instability is discussed in section 3.3. The uncertainties related with fault occurrence, fault type, fault location, fault clearing time and load level prediction are integrated in the probability expression. Section 3.4 gives a more developed estimation of the impact of transient instability. The risk calculation is summarized in section 3.5. In section 3.6, some preliminary work is presented towards a

method to calculate risk of transient voltage dip violation. This security problem is closely related with the transient instability phenomenon.

3.3 Probabilistic assessment of transient instability

The literature about this topic indicates that there are two fundamental ways to evaluate the probability of transient instability: the analytical method and Monte Carlo simulation.

3.3.1 Monte-Carlo simulation and analytical approaches

With a *Monte-Carlo process*, a simulation is performed where the uncertain parameters are modeled with known or assumed probability distribution function. There are two approaches: random approach and sequential approach. In the random approach, the simulation is repeated each time with new values for the random variables obtained from their respective distribution functions. In the sequential approach, the events are studied in a chronological succession, where the time of occurrence of a sample state is drawn at random. In order to obtain a sufficiently high accuracy, the number of simulations performed should be very high, or the simulation study period sufficiently long. Especially, when the number of uncertain parameters becomes large, then this approach becomes very time consuming. In an operation environment, the speed factor is indeed important and that is why in this work, analytical approaches are preferred.

There are different ways to model the uncertain parameters analytically. With a pure analytical method the probability distribution function of the uncertain parameter is obtained analytically from the probability distribution function of another parameter from which it depends and whose probability function is known. This is possible if the function between the two parameters is known. It corresponds to a random variable space transformation. If this function is not known, than another analytical method can be used: the conditional probability method. It is in fact a simulation method but where the randomness of the Monte Carlo simulation has been replaced by a deterministic simulation. The function between the

two parameters will be approximated by a set of simulations. The conditional probability of instability is calculated through simulation for every given set of uncertain parameter values. The total probability is then obtained by integration or summation of conditional probability over all possible values of the uncertain parameters.

In this work, analytical methods are used: a conditional probability of instability for the next period (next hour) is calculated for one operating point considering the uncertainties related with the fault occurrence (occurrence rate, type, and location). On the other hand, assuming a known probability density function (pdf) for the fault clearing error and load level uncertainty, these pdf's can be transformed analytically into a density function for the stability index φ.

In this probabilistic approach, it is assumed that the protection system is operating correctly: breaker failure is not considered. The event that a fault is not properly cleared may be a severe disturbance, but the probability of this event is so low that it would barely affect the risk value. This has been shown in [45]. The system configuration is assumed to be known. The following notation will be used: a fault is uniquely defined by the following variables: circuit C, location L_c on C, fault type F, clearing time τ and system load level P_L. It is also assumed that these variables are independent.

3.3.2 Expression for probability of instability

In this subsection, the probability of transient instability is derived from the probabilistic modeling of the fault and system uncertainties. The uncertainties in fault occurrence, fault type and fault location are represented by a discrete probability distribution function, which allows the calculation to be automated in a structured fashion. It has already been demonstrated earlier in Table 3-1, that variation in these parameters have considerable influence on the generation limit. The conditional probability of instability with only these uncertain parameters is presented in sections 3.3.2.1-3.3.2.4. The uncertainty of the fault clearing time and the pre-fault load conditions are included using the random variable transformation, as described in sections 3.3.2.5-3.3.2.7.

3.3.2.1 Fault occurrence

Each line has a fault rate that can be modeled by a Poisson distribution with a line outage rate λ_c. This is justified because the probability model of component failure is equivalent to the model of the time to the next failure[2] and typically, the random variable *time to next failure* is modeled by an exponential distribution. The reciprocal of this random variable, the number of faults over a period of time, is modeled by a Poisson distribution with parameter λ, being the fault rate. The fault rate can be obtained from historical data. Since it is assumed that the line will be outaged for several hours following the fault, a line can only be faulted once over the next period (next hour). Therefore, only the probability that one fault will occur over the next period is of interest. The probability of having two lines faulted over the next period is negligible. The expression for the probability of having a fault on line C is:

$$\Pr(C = c) = \Pr(N = 1 \mid \lambda_c) = \left. \frac{e^{-\lambda} \cdot \lambda_c^N}{N!} \right|_{N=1} = e^{-\lambda_c} \lambda_c \tag{3-1}$$

In the deterministic approach, it is simply assumed that the fault will occur with probability equal to one.

3.3.2.2 Fault location

To account for the influence of fault location on the probability of transient instability, a discrete uniform distribution is assumed for the fault location. According to the Bayes-Laplace criterion, the uniform distribution should be used if not enough evidence is available that one particular distribution is more valid over another. This is the case here: very little historical information is available on the locations of the faults on the lines, so it is fair to assume that roughly every location on a line has the same probability to be struck by a fault. A more refined assessment of the fault location probability could be performed by analyzing the geographical conditions of the area through which each line passes: in a forested area, the lines can be touched by the tree branches, an overhead line through an open area has a larger probability to be struck by lightening than a line through an urban area. Therefore, any appropriate distribution can be used if there is enough evidence pointing

[2] It gives the probability that a given number of faults will occur over a certain time period.

towards the corresponding probability pattern along the line. The probability of having a fault on location L_c of circuit C, given a fault occurs on circuit C, is given by

$$\Pr(L_c = l \mid N_c) = \frac{1}{N_c} \tag{3-2}$$

where N_c is the number of segments in which line C is divided. The percentage of segments leading to instability for a given fault type determines the conditional probability of instability.

In the deterministic approach, it is assumed that the fault will occur at the generator terminals with probability equal to one.

3.3.2.3 Fault type

The event space consists of four fault types F corresponding to mutually exclusive events. They are listed in Table 3-2 in descending order of severity: three phase to ground, two phase to ground, line-to-line and single phase to ground. Other fault types have either a negligible probability of occurrence or a negligible impact, or both. The severity of the fault is measured by the value of the fault impedance; the smaller the impedance, the larger the accelerating power, and the more likely the unit will lose synchronism. The fault impedance is expressed in terms of the negative and zero sequence impedance, Z^{neg} and Z^{zero} as shown in Table 3-2. In this approach, only the effect on the positive sequence network is considered. The values of the fault impedances should be calculated at every new operating condition, new topology and for each fault location.

Table 3-2. Fault impedances for each fault type

n	***Fault***	***Impedance***
1	3 phase	0
2	2-phase	$\frac{Z^{zero} \cdot Z^{neg}}{(Z^{zero} + Z^{neg})}$
3	Line-line	Z^{neg}
4	Single phase	$Z^{neg} + Z^{zero}$

From historical data we can obtain the frequency f_n of occurrence of each fault type given a fault occurs on the line $F=n$ for a particular line, from which then the probability of occurrence is derived (3-3).

$$\Pr(F=n)=\frac{f_n}{\sum_{j=1}^{4} f_j} \text{ for n=1 to 4} \tag{3-3}$$

In the deterministic approach, a three-phase-to-ground fault is assumed with probability one.

3.3.2.4 Probability of instability I

The event of transient instability denoted as K_s is the event where the unit at risk is losing synchronism and is disconnected. To calculate the probability of K_s the law of Total Probability is applied. The idea behind this law is illustrated with the following example. From Figure 3-1, it can be seen that the event A can occur simultaneously with each one of the B_i events (i = 1 to n). The probability of event A is equivalent to the summation of the intersections of A with the individual B_i's or:

$$\Pr(A)=\Pr(A\cap B_1)+\cdots+\Pr(A\cap B_n) \tag{3-4}$$

Given that $\Pr(A\cap B_i)=\Pr(A\mid B_i)\cdot\Pr(B_i)$, equation (3-4) can now be rewritten as follows:

$$\Pr(A)=\sum_{i=1}^{n}\Pr(A\mid B_i)\cdot\Pr(B_i) \tag{3-5}$$

This expression can be very useful in case the terms conditional probabilities and the marginal probabilities $\Pr(B_i)$ are easier to obtain than $\Pr(A)$ directly. This occurs in the transient stability case discussed in this work. The event A represents the instability event K_s, and B_i is the fault occurrence event, which consists of the probability of three independent random variables, C, L_c, and F. Now, the probability of the event K_s of having a generator losing synchronism is given by equation 3-6.

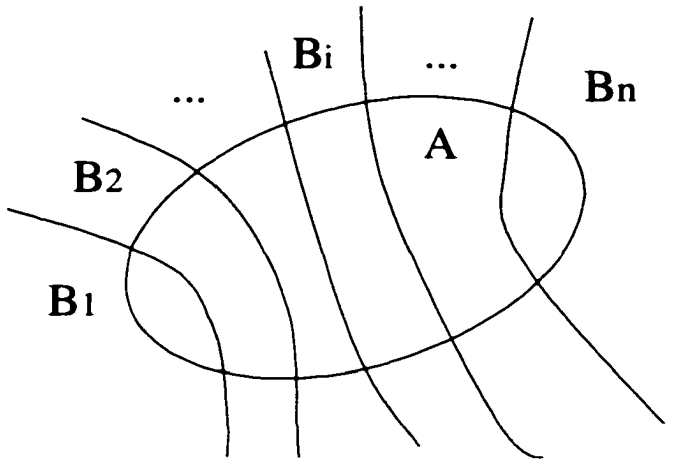

Figure 3-1. Law of Total probability

$$\Pr(K_s \mid \bar{x}) = \sum_{c=1}^{N_L} \sum_{l=1}^{N_c} \sum_{n=1}^{4} \underbrace{P(K_s \mid C=c, L_c=l, F=n, \bar{x})}_{I} \cdot \underbrace{\Pr(C=c) \cdot \Pr(L_c=l) \cdot \Pr(F=n)}_{II} \qquad (3\text{-}6)$$

The first term (*I*) in the summation, is the conditional probability of instability. If only fault rate, fault type and fault locations are modeled probabilistically, this term only takes two values: one or zero, depending on whether an instability event is detected at these conditions or not. The term *II* represents the joint probability of the fault conditions: it is the product of the probability of circuit c being faulted, the probability of the fault on circuit c being at location l, and the fault being of the type n, respectively (3.3.2.1-3.3.2.3). Equation 3-6 shows that a stability assessment has to be performed for every fault type and location condition on every line considered. In the next two subsections, the uncertainties related with the fault clearing time and pre-fault load level are discussed. Only after the risk calculation has completely been developed, their influence on the risk index can be monitored. This will be done in chapter 4.

3.3.2.5 Fault clearing time

In Table 3-1, it was shown that the uncertainties dealt with so far were known to be influential on the transient stability performance of a system faced with a disturbance. A conditional probability of instability is provided in term *I* of equation 3-6, given a fault of a

certain type on a certain location on a certain line. With no other uncertainties involved, this probability is zero or one. The error on the clearing time is traditionally neglected in the deterministic approaches.

The time to clear a fault is the sum of the relay operating time and the circuit breaker tripping time. The operating times of these devices are both random. In reference [35], a more detailed approach is presented to model the protection system probabilistically. The density function for the clearing time is obtained from the convolution of the relay and breaker operating times. In this work, the clearing time distribution is approximated by a normal distribution around the supposed clearing time.

According to the information provided by some breaker manufacturers, the error on τ can go up to 10% or even 1 cycle longer than the designed time. The error on the lower side of the designed time is a little larger. This uncertainty is modeled here with a normal distribution, with 0.1s mean and a 10% or 16.666%[3] standard deviation.

When previously the system suffering a fault type–location combination was very close to the stability boundary, the conditional probability was either zero or one, depending on which side of the boundary it was. On the other hand, a small error on the fault clearing time τ can make the system cross this boundary. Consequently, acknowledging the fault clearing uncertainty and modeling it probabilistically would lead to conditional probability values between zero and one.

In chapter 2, an index φ is presented to measure the degree of instability, taking positive values for stable cases, and negative for unstable cases. The value of the stability index φ clearly depends on the clearing time τ. This functional dependency is denoted as f according to:

$$\varphi = f(\tau, C, L_c, F)$$

where the other fault parameters C, L_c, and F are specified.

---

[3] One cycle is 16.66% of the mean clearing time 0.1s

According to the method described in section 2.2.4, a negative value of φ represents transient instability. Therefore, given the distribution function of τ, the probability of instability (term *I* of equation 3-6) corresponds to the probability of $\varphi < 0$. All probability expressions are conditioned on the fault parameters, but the corresponding notations are omitted to avoid unwieldy expressions.

$$\begin{aligned} \Pr(K_s / C = c, L_c = l, F = n, \bar{x}) = \Pr(\varphi < 0) &= \Pr(f(\tau) < 0) \\ &= \Pr(\tau > f^{-1}(0)) \\ &= \Pr(\tau > \tau_{cc}) \\ &= \int_{\tau_{cc}}^{\infty} \frac{e^{\frac{(\tau-\bar{\tau})^2}{2\sigma_\tau^2}}}{\sqrt{2\pi\sigma_\tau}} d\tau \\ &= \Phi\left(\frac{\tau_{cc} - \bar{\tau}}{\sigma_\tau}\right) \end{aligned} \qquad (3\text{-}7)$$

Here, $\bar{\tau}$ is the mean (designed) clearing time, and σ_τ is the standard deviation, and τ_{cc} the critical clearing time. This calculation actually only requires the computation of τ_{cc}, since the values for $\bar{\tau}$ and σ_τ are assumed. In equation 3-7, the equality sign changes from < to > because the function *f* is monotonically decreasing.

3.3.2.6 Load level uncertainty

Another parameter that can influence the stability behavior of a generator and thus the risk value is the load level. When the risk level is calculated on a one-hour-ahead basis, the accurate load level values might not be predicted correctly. A multivariate normal distribution with a 2% standard deviation for a one-hour-ahead load level prediction is assumed. Two extreme situations are distinguished here: perfect linear correlation between load levels and no linear correlation between the load levels. The first case corresponds to a correlation factor equal to one: all loads change proportionally with the same factor. It is actually a pessimistic case, because it means that all individual loads increase together, having more impact on the generator levels and thus on the stability. The other extreme is when the correlation factor is zero. In this case, the load changes have a smaller effect on the

stability because the various changes are compensated by one other. Since the first case represents a more severe situation, the analysis is limited to this one. Only the worst case will be analyzed here. The inclusion of this uncertainty is similar to the previous case. The functional dependency g of the stability index with the total load level P_L is established, given that the other fault parameters are kept constant:

$$\varphi = g(P_L, C, L_c, F)$$

The probability of instability with uncertain load level is given by:

$$\begin{aligned} \Pr(K_s / C = c, L_c = l, F = n, \bar{x}) = \Pr(\varphi < 0) &= \Pr(g(P_L) < 0) \\ &= \Pr(P_L > g^{-1}(0)) \\ &= \Pr(P_L > P_{Lc}) \\ &= \int_{P_{Lc}}^{\infty} \frac{e^{\frac{(P_L - \bar{P}_L)^2}{2\sigma_L^2}}}{\sqrt{2\pi\sigma_\tau}} d\tau \\ &= \Phi\left(\frac{P_{Lc} - \bar{P}_L}{\sigma_L}\right) \end{aligned} \qquad (3\text{-}8)$$

where $\bar{P}_L$ is the predicted load level and σ_L, the standard deviation, and P_{Lc}, the critical load level.

In the case that a longer period of observation is considered, the standard deviation on the load prediction will also increase, and the above assumption (total load dependency) is no longer valid. In that case, the covariance or the correlation factor for the multivariate normal distribution of the load levels should be obtained from historical data. A multivariate normal distribution of the load levels is commonly accepted in probabilistic stability studies [32][42], although in [41] a discrete probability modeling has been used to represent the stochastic nature of the load levels.

3.3.2.7 Probability of instability II

If the error on the clearing time and the load level prediction are considered, term *I* in equation 3-6 can further be rewritten, assuming a bivariate normal distribution for the clearing time and load level:

$$P(K_s \mid C = c, L_c = l, F = n, \bar{x}) = \int_{\tau_{cc}}^{\infty} \int_{P_{Lc}}^{\infty} f(\tau, P_L \mid C = c, L_c = l, F = n, \bar{x}) d\tau \cdot dP_L \qquad (3\text{-}9)$$

Note that there is a dependency between τ_{cc}, the critical clearing time and P_{Lc}, the critical load level.

3.4 Impact/Damage assessment

The second component of risk is the impact or cost consequence. The impact is very system specific, so a general approach is identifying all possible costs of instability and the entities incurring these costs is presented. In chapter 4, this perspective will be narrowed to that of the generator owner.

A transient instability event causes the generator to accelerate and go out-of-step. The power produced by the The overspeed protection will act to protect the generator circuits against large electromagnetic forces. The unit will be tripped and will remain out of service for a period time. In this study, the length of this period is taken as the average down time of the unit, or also referred to as the *mean-time to repair* (MTTR). During this time, the machine needs to be inspected and may need some maintenance and repair, especially at the windings and at the insulation which could have been damaged.

The costs associated with a transient instability are divided into three categories:

I. *Generator repair and start-up costs - Im_{start}*

After an out-of-step condition the generator is taken off-line for a repair and maintenance – repair costs c_{rep}. A certain amount of effort and fuel must be used to bring the unit back on-line: this cost is called *start-up* costs c_{start}.

$$Im_{start} = c_{rep} - c_{start}$$

II. *Opportunity cost - Im_{op}*

When a unit is taken out of service the lost generation needs to be picked up by another, probably less efficient generator having a higher fuel cost rate. Depending on the operation context, several scenarios can happen. In case the owner of the disconnected unit still has enough reserves to pick up the lost generation, the cost will be merely an economic dispatch cost difference. If the lost generation has to come from another supplier, the owner of the lost unit will lose the revenue from the power it was supposed to deliver, with a possible penalty. He also might buy the lost power from another generation company: in that case, the cost will be the difference between the purchase cost and the production cost.

This cost is calculated as follows:

$$Im_{op} = (C_{new} - C_{old}) \cdot h \cdot P_{lost}$$

where C_{new} is the cost per MWhr during the outage, and C_{old} is the cost per MWhr prior to the outage, h is the duration of the outage, and P_{lost} is the amount of generation that the tripped unit was supplying.

III. *Loss of load - Im_{load}*

Tripping a generation unit will initially cause a deficit in power supply over the system, causing the frequency to drop. If the frequency drops below a certain level for a specified amount of time, an under-frequency load shedding relay will activate some breakers to interrupt a pre-set block of load. The amount of load that will be shed for a given fault depends on the relay settings. This impact is especially system dependent.

The cost of the loss of load is calculated by multiplying the amount of shedded load by the per MWhr penalty factor C_{pen} and the duration h.

$$Im_{load} = C_{pen} \cdot h \cdot P_{shed}$$

IV. *Penalties for reliability criteria violation - Im_{viol}*

NERC is poised to implement "compliance measures" that identify economic penalties for violating reliability criteria.

V. *Cascading events - Im_{viol}*

These are very difficult to quantify, but potentially large.

The total impact is the sum of the three types of costs:

$$Im(K_S \mid \bar{x}) = Im_{start}(K_S \mid \bar{x}) + Im_{op}(K_S \mid \bar{x}) + Im_{load}(K_S \mid \bar{x}) + Im_{viol}(K_S \mid \bar{x}) + Im_{casc}(K_S \mid \bar{x}) \quad (3\text{-}10)$$

3.5 Overview of the risk calculation methodology

With the probability of instability defined in section 3.3, and the impact described in section 3.4, the risk is calculated as the product of both. Since risk is actually the expectation of the impact, the procedure above can also be interpreted as the development of a probability mass function for the random variable impact *Im*. Indeed, the impact has a Bernouilli distribution function with probability *p*. The complete algorithm for risk of transient instability calculation is shown in Figure 3-2.

The probability *p* is the total probability of instability expressed by equation 3-6 together with equation 3-9. With a Bernouilli distribution function (Eq. 3-11), the expected value E[Im] of the impact is obtained as shown in Eq. 3-12.

$$Im \sim Bernouilli(p) \qquad \mathrm{Im} = \begin{cases} I & p \\ 0 & 1-p \end{cases} \quad (3\text{-}11)$$

$$Risk(K_s \mid \bar{x}) = E[\mathrm{Im}] = I \times p + 0 \cdot (1-p) = I \times p \quad (3\text{-}12)$$

In order to obtain system-wide risk of instability when different machines are at risk of going out-of-step, the procedure is repeated for each one of the at-risk generators and the sum of all individual risks will give the total system risk.

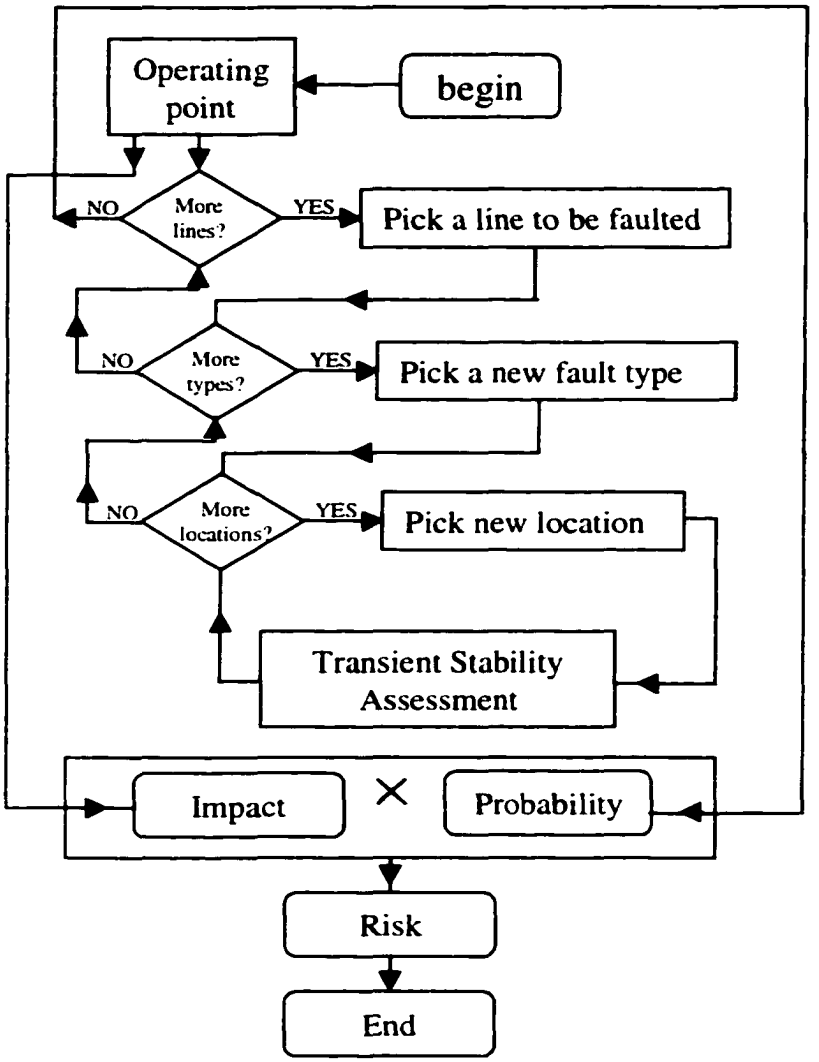

Figure 3-2. Transient instability risk calculation overview for one operating point.

3.6 Voltage Dip Assessment

The transient behavior of power systems does not only depend on whether angle instability occurs or not. After a large disturbance, the system will experience rotor angle swings, causing the voltage to fluctuate at various buses and possibly drop to dangerously low voltage levels. This insecurity problem that is related to the transient instability phenomenon, has received a lot of attention from the utilities because of its potentially severe consequences. In this section, some preliminary work is presented of a methodology to

calculate the risk of voltage dip violation. Expressions for the probability and impact of voltage dip violations are presented. However, additional work is required to work out the details of the method, as well as to implement the method and to find ways to reduce its computational effort.

If the voltage dip is significant in magnitude and duration, some under-voltage protection relays may trip large induction motors and industrial drives, possibly causing substantial damage to industrial processes, even if no angle instability has occurred. In particular, in nuclear power plants a significant voltage dip can be interpreted by the protection equipment as a loss of coolant, leading to the whole unit being tripped [47]. It is for these two reasons that transient stability reliability criteria also include a performance limit associated with transient voltage dips. Depending on the types of load connected to a system, the voltage dips should not be deeper than a certain limit (15, 20% of the nominal value) and not for more than a certain time (in transmission level 0.05s, 0.15s). This performance requirement can be sometimes more restrictive than the angle stability requirements.

According to Debs [50], the maximum voltage dip in the system will occur at the point where the transient potential energy also is at its maximum. At this point, the angular separation between the critical machines and the rest of the machines is maximal. Since, at this condition, the machine voltage magnitudes are out of phase with each other, it is argued that the bus voltage magnitudes will dip to their lowest levels.

The problem here will be the assessment of the voltage dip either in time, as in duration. Using time-domain simulation will be very time-consuming. In the literature, the use of TEF methodology was proposed to find the angle where the maximum voltage drop occurs [48]-[52]. In [53] the use of ANN was suggested to predict both the voltage dip and the dip duration.

3.6.1 Risk-based approach

As in the previous risk assessment approaches, the probability and impact of the voltage dip violations needs to be calculated. A voltage dip assessment methodology needs to

be specified, in the same way a transient stability assessment tool is used in the transient stability risk approach.

When assessing the impact of voltage dip violation, it is necessary to evaluate both the magnitude of the dip as well as the duration of the dip below a limit value. Most loads are protected against under or over voltage by protection relays. The operation of this protection system is dependent on the composition of the load at that bus. Some loads are more sensitive than others to voltage dips and have a narrow voltage toleration band.

The event of transient instability will either occur or will not occur, and the cost consequences when instability occurs is assumed to be only dependent on the operating conditions, not on the fault conditions. On the other hand, voltage dips occur with different severity in terms of magnitudes and durations, and the consequences of voltage dips depend on this severity as well as the load mix affected by the voltage dip. In addition, they also depend on the fault conditions. In other words, where transient instability is a discrete event, voltage dip is continuous, and probabilistic modeling must reflect this difference.

For a given fault condition (line, location on line and type), the voltage dip profile at each bus needs to be evaluated. Voltages reach their lowest level at some time after the fault is cleared. The duration is measured as the time the voltage magnitude remains below a certain limit. Since the voltage dip magnitude and the duration limit depend on the composition of the load connected at the bus at the moment of the fault, it is difficult to determine these limits precisely, and they are therefore considered to be random variables and their probability density functions can be estimated through simulation using statistics for load voltage sensitivities.

The objective is to obtain the expected value for the impact caused by the voltage dip violation. The deeper the dip, the more important will be the consequences, the more load will be shed. As opposed to the transient stability term where the impact incurred was either total or zero, here the impact is dependent on the extent (in terms of magnitude and duration) of the violation, and that is why it is referred to as the *expected* impact.

3.6.1.1 Probability of voltage dip violation

With a measure for the voltage dip magnitude at a load bus b, probability density functions $f_{v,b}(v_{\text{lim}})$ and $f_{t,b}(t_{\text{lim}})$ are used for the voltage magnitude lower limit and the

duration upper limit at bus *b*, respectively. The probability of the voltage dip being lower than the lower limit, regardless of the duration is given by:

$$\Pr(v_{dip}) = \int_{v_{dip}}^{\infty} f_{v,b}(v_{\lim})dv_{\lim}$$

The event of load being interrupted at bus *b*, because of a voltage dip violation in magnitude and duration is denoted as the event $K_{v,b}$. This event occurs if the voltage magnitude remains below the limit long enough to activate the protection relays. This is illustrated in Figure

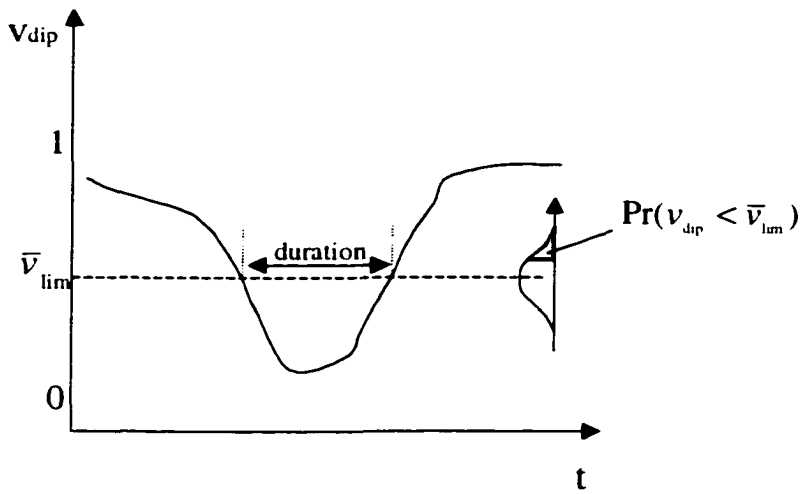

Figure 3-3. Voltage dip magnitude and duration

The probability of the event $K_{v,b}$ given a fault of a specific type occurs at a specific location is given by the following expressions:

$$\Pr(K_{v,b} \mid C = c, L_c = l, F = n, \overline{x}) = \Pr(t > t_{\lim} \mid v_{dip} < v_{\lim})$$

$$\Pr(K_{v,b} \mid C = c, L_c = l, F = n, \overline{x}) = \int_{v}^{\infty} \int_{0}^{t(v_{\lim})} f_{v,b}(v_{\lim}) f_{t,b}(t_{\lim}) dt_{\lim} dv_{\lim}$$

The magnitude and duration limits are here assumed to be independent. However, strictly speaking, the time that the voltage magnitude remains under a certain level depends on this level, which is a random variable. This explains why the upper limit of the second

integral has the dependency on the magnitude explicitly indicated. To simplify the calculation, the integral upper limit can be assumed dependent from the mean voltage dip limit $\bar{v}_{lim}$ instead of the voltage dip limit v_{lim} itself.

3.6.1.2 Expected impact of voltage dip violation

If load is interrupted, it is assumed that the load D_b at bus b is disconnected. The expected impact at bus b is obtained by multiplying the amount of interrupted load with the per unit cost C_b of interrupted load and the probability computed with equation 1:

$$E(\mathrm{Im}(K_{v,b} \mid C = c, L_c = l, F = n, \bar{x})) = \Pr(K_{v,b} \mid C = c, L_c = l, F = n, \bar{x}) \cdot C_b \cdot D_b$$

This expression emphasizes the fact that the deeper the voltage dip and the longer the violation lasts, the more load will be dropped. Instead of only considering shedding all load at a bus at once, the method can be refined by treating at each bus the different load categories in different ways considering different pdf's for the limits, as suggested in reference [99]. The expected impact over all load buses given the fault, is obtained by summing the individual impacts: K_v is now defined as the event where voltage dip violation occurred somewhere in the system.

$$E(\mathrm{Im}(K_v \mid C = c, L_c = l, F = n, \bar{x})) = \sum_b E(\mathrm{Im}(K_{v,b} \mid C = c, L_c = l, F = n, \bar{x}))$$

Finally, the risk of voltage dip violation is computed through the following expression:

$$Risk(K_v \mid \bar{x}) = \sum_{c=1}^{N_C} \sum_{l=1}^{N_L} \sum_{n=1}^{4} E(\mathrm{Im}(K_v \mid C = c, L_c = l, F = n, \bar{x})) \qquad (3\text{-}13)$$

3.6.1.3 Overview of the calculation methodology for risk of voltage dip violation

To summarize the presented algorithm to calculate risk of transient dip violation is shown in Figure 3-4.

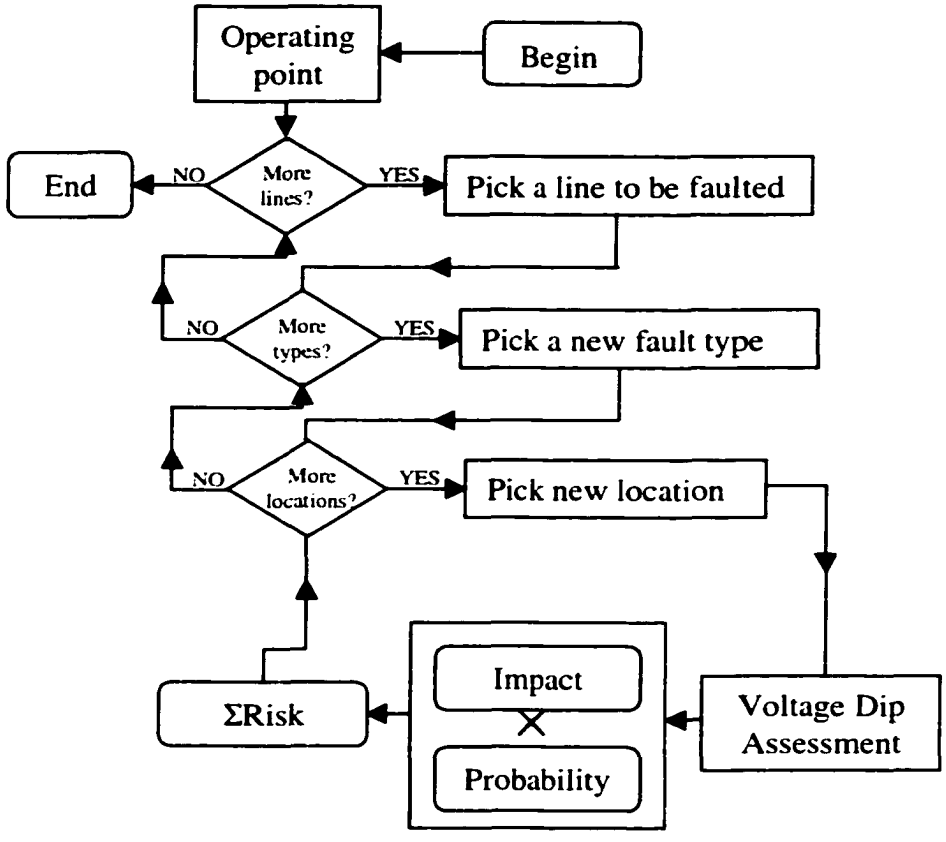

Figure 3-4. Transient instability risk calculation overview.

3.7 Summary of the chapter

In this chapter, the conservativeness of the deterministic transient stability limits is illustrated through an example. The complete probability calculation procedure is developed indicating how fault occurrence, fault type, fault location, fault clearing time and pre-fault level uncertainty is included, and the impact of angle instability is quantified. Finally, some preliminary work is presented towards a framework to calculate the risk of voltage dip.

4. RESULTS ON TEST CASE

This chapter illustrates the methodology to calculate risk of transient instability presented in the previous chapter. An operating scenario within the IEEE RTS '96 test system is used for this illustration.

In section 4.1, the test system is presented and section 4.2 describes the software developed for this research. Section 4.3 provides an overview of the parameter values used in the risk calculations. Section 4.4 illustrates the influence on the risk uncertainty in fault clearing time and load level. Section 4.5 provides examples of how risk levels vary with certain operating parameters.

4.1 Test system

The test system used in this work is a modified version of the IEEE Reliability test system – 1996 [54]. The one-line diagram is shown in Figure 4-1. The modifications from the original system are summarized below:

- Line 11-13 has been taken out for scheduled maintenance.
- At the bus 23 plant, the 350MW unit has been replaced by a 155 MW unit
- The fault rate of the line 13-23 has been doubled.

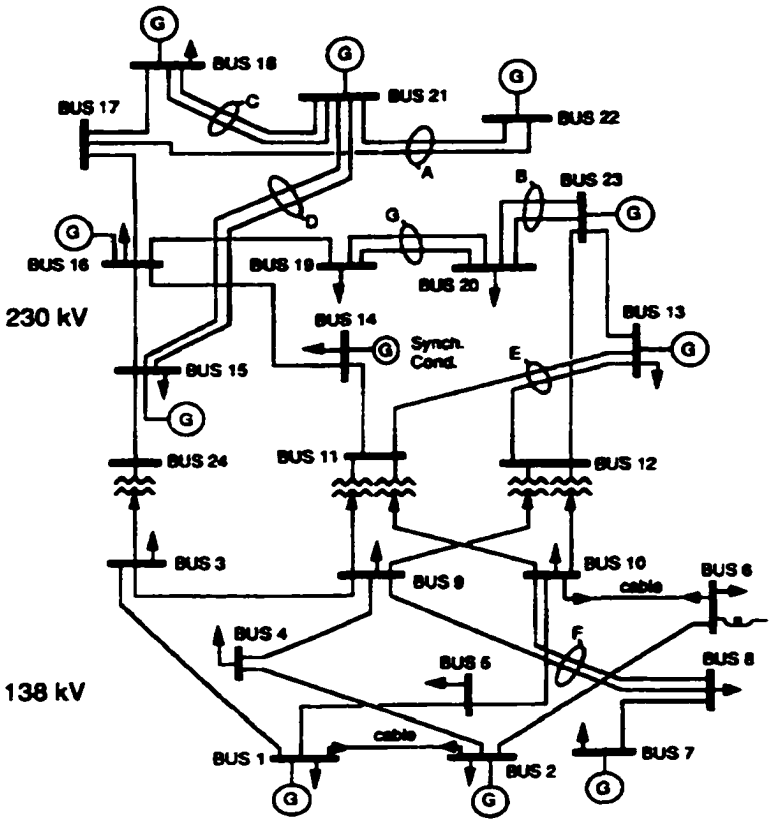

Figure 4-1. One-line diagram of the IEEE 24 bus RTS system

4.2 Developed software

A software module was developed to calculate risk for any pre-fault operating conditions or any range of operating conditions. The software consists of a main controlling batch-file monitoring several industry grade software modules: a load flow calculation (IPFLOW), and a transient stability simulation program (ETMSP) and its output analyzer (OAP)[4].

The software has three parts;

1. Pre-fault operating conditions: the input file for the risk-calculation module can be set and modified through the IPFLOW interface.

[4] EPRI software, on a Hewlett-Packard C110-9000 125MHz and 64Mb RAM processor

2. Risk calculation module: for a desired range of pre-fault conditions, the risk calculation algorithm will initiate three cycles, one for all considered faulted lines, one for the locations on that line and one for the fault types. For each line/location/type combination, the Transient Stability Index is calculated using ETMSP and OAP.
3. After all cycles are completed, the risk is computed and stored in a file that can be used to be plotted with MATLAB or any other graphic tool.

To obtain the results presented in this work, the early termination method described in section 2.1.4 was not applied, because the source code of the simulation software could not be changed. Only classical machine models were used. However, the methodology is capable of accommodating any type of machine modeling.

In parallel, a MATLAB prototype with graphical user interface was developed for demonstration purposes only, calculating risk of instability. In this case early termination was used and a simple trapezoidal numerical integration to solve the differential equations. However, it applies only to classical machine modeling.

4.3 Parameter values for risk calculations

4.3.1 Probability

Fault occurrence

Instability of the plant at Bus 13 can only be caused by faults on either one of the two lines emerging from that bus. Table 4-1 gives the probabilities of either line being outaged. Faults on the other lines were previously tested and did not cause any instability of the units at Bus 13 under any circumstances, and therefore they are not considered here.

Table 4-1. Occurrence probability of line outages

Line outage	*Probability /hr*
13-12	4.58E-5
13-23	9.16E-5

Fault type

From historical data, the following probabilities were obtained. Other types of faults were not considered, either because their probability of occurrence or severity, or both is negligible.

Table 4-2. Occurrence probability of fault type

Fault type	*Probability*
3 phase-to-ground	0.062
2 phase-to-ground	0.10
Single phase-to-ground	0.75
Line-to-line	0.088

Fault location

A discrete uniform distribution is adopted where each one of the two lines are divided into 10 segments. This means that 11 locations on each line are considered.

Clearing time

The fault clearing time is assumed to follow a normal distribution with mean 0.1 s and 15% standard deviation.

Pre-fault load level

The one-hour ahead pre-fault load level prediction is assumed to follow a normal distribution with the predicted load as mean and with a 2% standard deviation.

4.3.2 Impact

The values of each impact parameters are listed in Table 4-3. The penalties for reliability criteria violation and the cost associated with eventual cascading events are not included.

Table 4-3. Impact parameters

Repair and start-up costs: c_{rep} and c_{start}	$36,224 and $45,000
Outage duration h	10 hrs
Outage per MWhr cost C_{new}	68.5 $/MWhr
Original per MWhr cost C_{old}	29.95 $/MWhr
Load shedding cost C_{pen}	1,000 $/MWhr

4.4 Influence of uncertainties on Risk

In Table 3-1, the effect of uncertainty on fault occurrence, type and location on the generation limit is shown and it was observed that there are highly influential factors determining the transient stability performance of a system at a given operating point. Here the effect of uncertainty in clearing time and pre-fault load level on generation limits is analyzed. To do this, first, the risk of transient instability is plotted versus the generation level at plant 13. For this plot, only three uncertainties are considered: occurrence, type and location. The level of real power supply of the generator at risk of going unstable is clearly a determining factor for the stability. The higher the power output, and thus the mechanical torque, the higher the accelerating power during the fault. Subsequently, the unit will go out-of-step faster when the supply is higher, as shown in Figure 4-2.

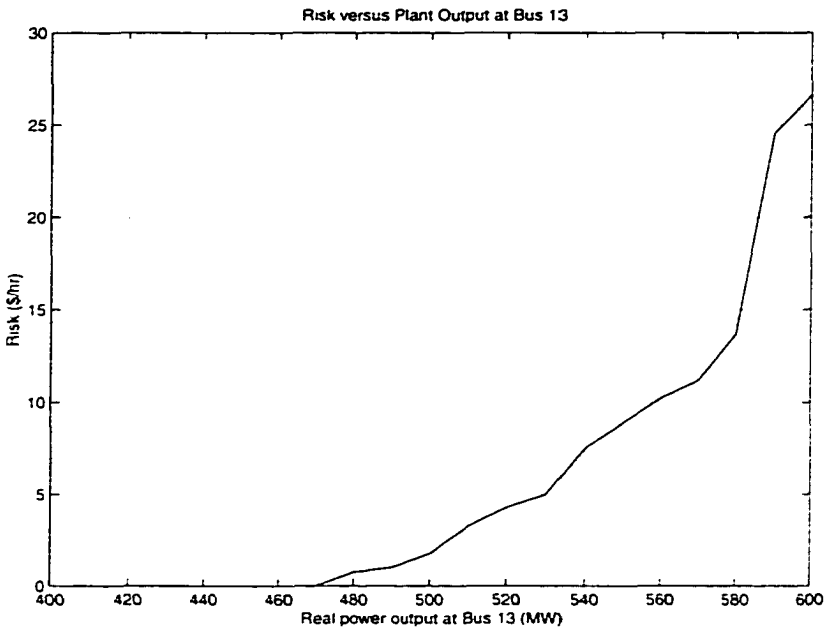

Figure 4-2. Generator level unit at risk.

From the plot, it is shown that with only these three uncertainties, the deterministic limit corresponds exactly with the point above which the risk is non-zero. This plot will be used as a reference in the next subsections to identify the influence of the uncertainties on the risk.

4.4.1 Uncertain clearing time

As explained in section 3.3.2.5, the actual fault clearing time can also be considered a random variable with an assumed normal distribution around the designed clearing time. The error on the clearing is traditionally neglected in the deterministic approaches.

To evaluate the effect of the clearing time uncertainty on the risk, the 95% confidence intervals are plotted next to the original plot shown in Figure 4-2. The result is shown in Figure 4-3. The upper curve corresponds to the risk with a designed clearing time plus 2σ, and minus 2σ for the lower curve. It can be seen that the intervals are very wide and, therefore, the modeling of this type of uncertainty should not be neglected and should be included in the risk calculation.

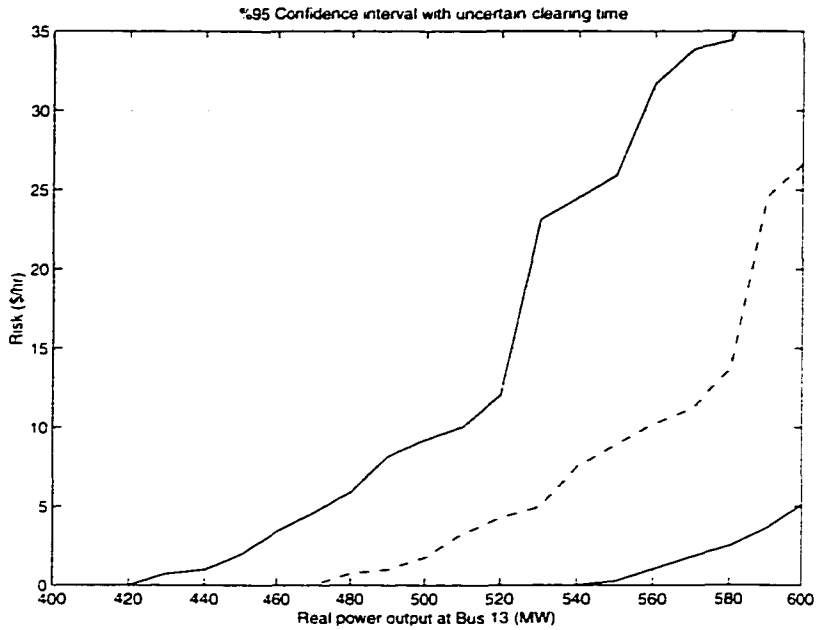

Figure 4-3. 95% confidence intervals with 15% uncertainty on the clearing time

The previous analysis establishes that fault clearing uncertainty can have a significant influence on the risk level, and that it consequently must be included in the risk assessment. Recalling the method presented in section 3.3.2.4, where the stability index $\varphi = f(\tau, C, L_C, F)$. We now seek to determine the function f.

Since there is no way to obtain this function analytically, it can be traced by a series of simulations combined with the bisection method, to find the exact clearing time for which the stability index becomes zero, i.e., the critical clearing time, τ_{cc}. Once this value has been determined, the probability of the index φ being smaller than zero can be calculated by $\Phi(\frac{\tau_{cc} - \bar{\tau}}{\sigma_\tau})$ (equation 3-7).

As an alternative to the more time consuming method, an approach is proposed that approximates the function f, by a piecewise linear function. Many different φ versus τ plots were obtained corresponding to different fault or operating situations, and some of them are presented below. The fault location is changed, the fault type, and a different generation levels are applied (Figure 4-4 - Figure 4-7).

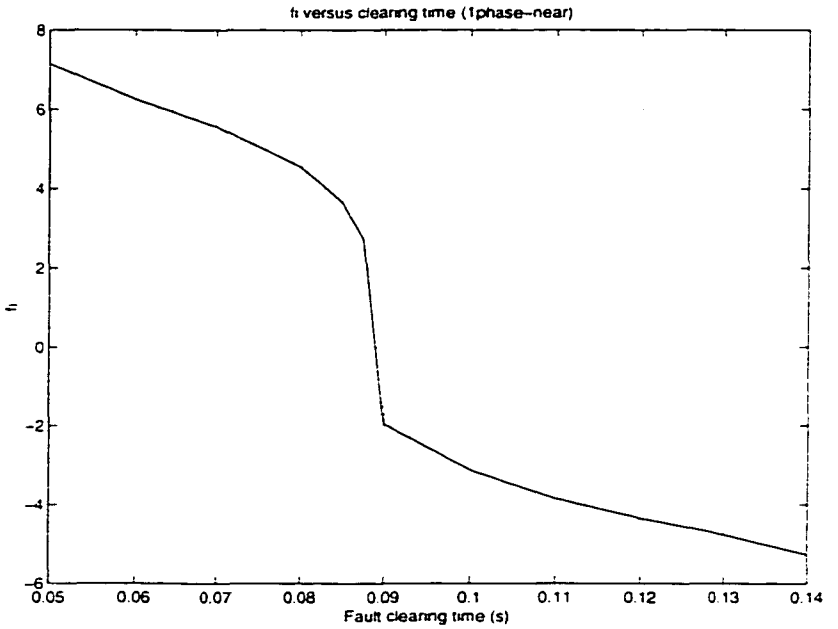

Figure 4-4. Three phase fault at near-end bus, P_{gen} = 600MW

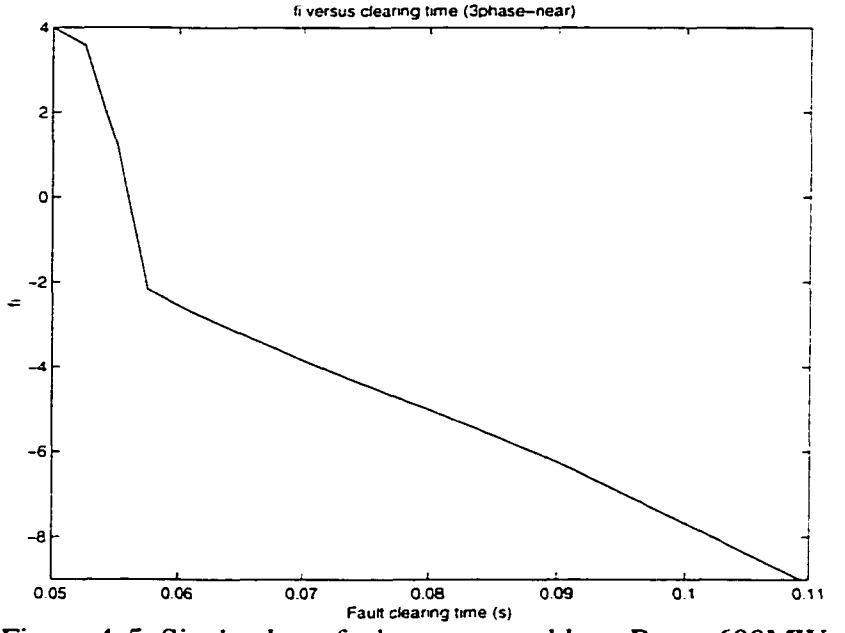

Figure 4-5. Single phase fault at near-end bus, P_{gen} = 600MW

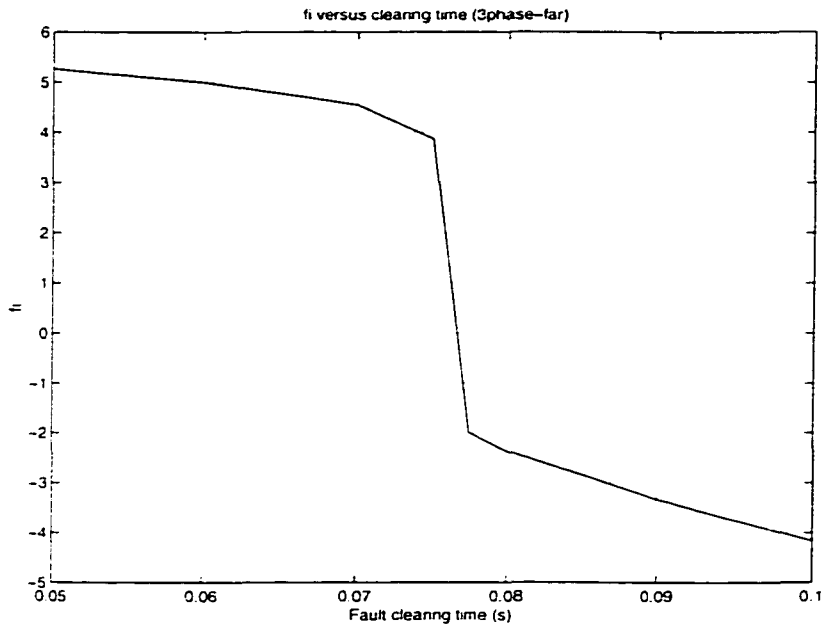

Figure 4-6. Three phase fault at far-end bus, P_{gen} = 600MW

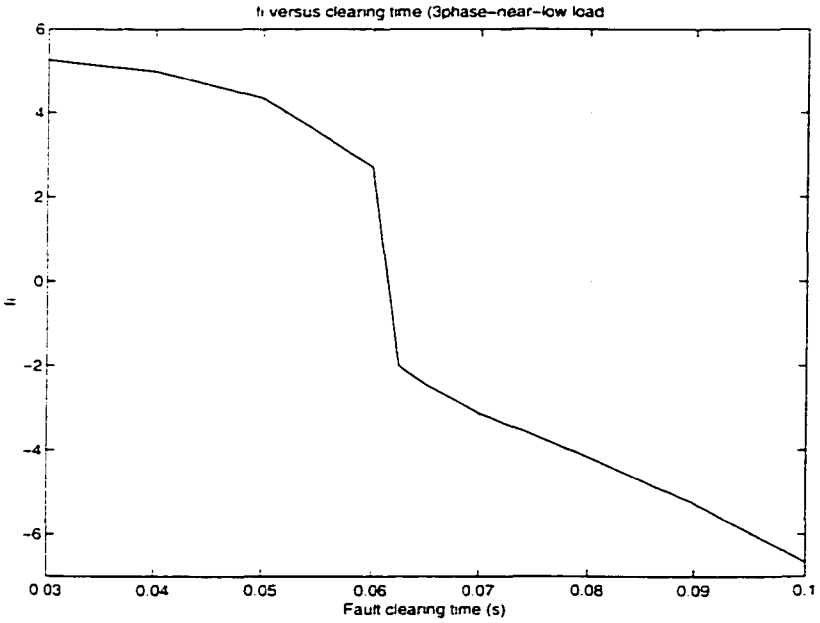

Figure 4-7. Three phase fault at near end bus, P_{gen} = 540 MW

From the four figures it can be seen that the curves can be approximated by a piecewise linear function. The function is monotonically decreasing such that the inverse of f can be defined as required in equation 3-7. Certain rules can be extracted from these plots: the corner points are always close to φ values of 2 and –2, and the slopes of the linear parts are also approximately constant. The approximated curve is illustrated in Figure 4-8: the shape of the curve is assumed constant, but its horizontal position is not known and depends solely on the φ value associated with the adopted clearing time.

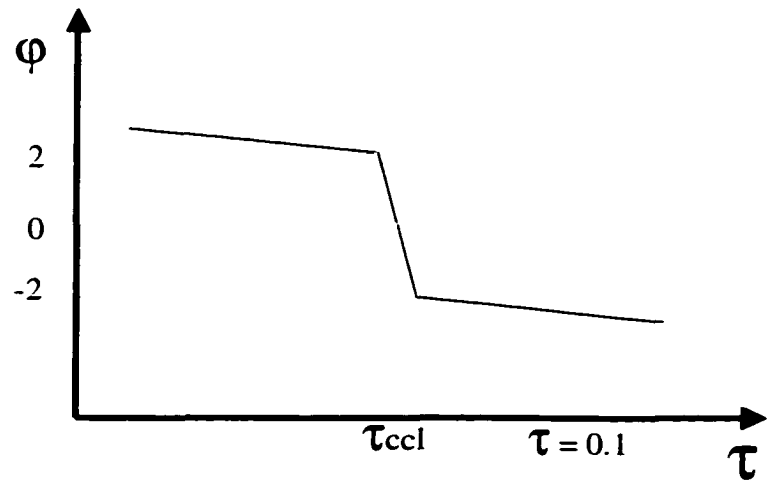

Figure 4-8. Approximated function between φ and τ

In order to calculate the probability of $\varphi < 0$, the probability of instability, the following steps are executed:

1. The φ corresponding to a clearing time of t = 0.1 is found, through transient stability assessment, according to the method presented in section 2.1.4.
2. Using the approximated function, shown in Figure 4-8, the critical clearing time τ_{ccl} is found. It corresponds to the clearing time for which φ is equal to zero (stability boundary). τ_{ccl} is the lower bound ($f^{-1}(\varphi = 0)$) of the integral in equation 3-7.
3. Finally, the result of the integral given in equation 3-7 is calculated and returns the requested probability value.

Error of approximation

The probability of instability error incurred by the adopted approximation for each one of the four cases presented in Figure 4-4 to Figure 4-7 is shown in

Table 4-4. The table shows that the errors in these cases are fairly small. However, the closer a case is to the stability boundary, the higher the approximation error will be. Nonetheless, it is believed to be a good enough to enable a rapid risk calculation. Figure 4-9 illustrates the effect of including the clearing time uncertainty on the risk. The dashed line is the original curve from Figure 4-2, with no clearing time uncertainty. From the Figure 4-10, it can be seen that for a range of about 40MW below the deterministic limit, the risk is small, but not completely zero. This shows that deterministic limit (at 470 MW) is not always conservative. In fact it can also be unsafe, as shown here.

Table 4-4. Probability of instability approximation error

	Estimated	*Correct*	*% error*
Three phase at close-end bus	1.000	1.000	0
Single phase at close-end bus	0.843	0.816	3.21
Three phase at far-end bus	0.982	0.985	0.22
Three phase near, lower generation	1.000	0.9999999	negl.

4.4.2 Uncertain load level

In this subsection the effect of pre-fault load level uncertainty on the risk is analyzed. A time horizon of one hour is used, for which it is usual to assume a 2% load level standard deviation. As explained in section 3.3.2.5, the worst-case scenario will be tested first, using a correlation factor of the loads among the buses equal to one. If the influence turns out to be minor, it indicates that the load uncertainty is not a factor when calculating the risk of transient instability in an operating environment. If the influence is relevant, a more detailed modeling of the load uncertainty needs to be adopted. Figure 4-11 is the same as the risk versus generation level depicted in Figure 4-3, but this time the 95% confidence interval [-2σ/+2σ] is shown corresponding to the 2%

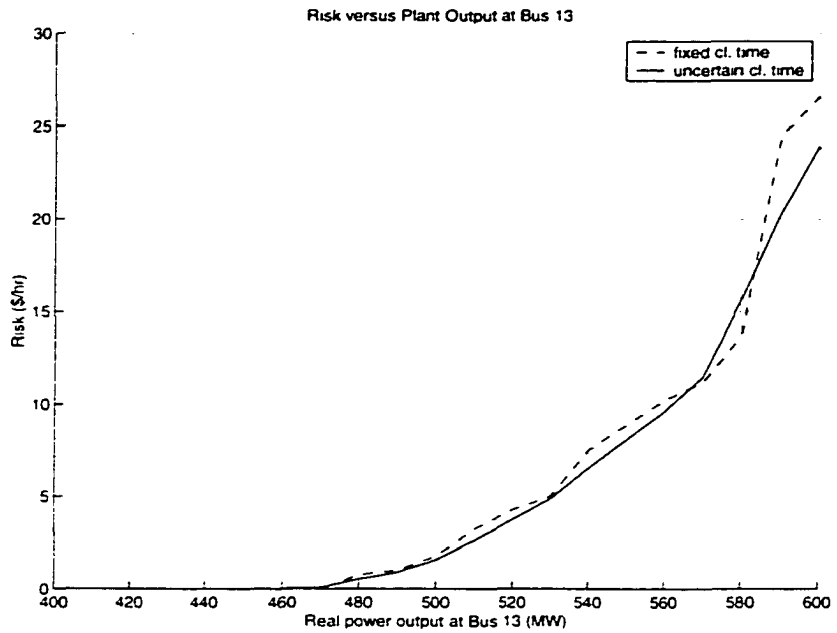

Figure 4-9. Influence of clearing time uncertainty on risk

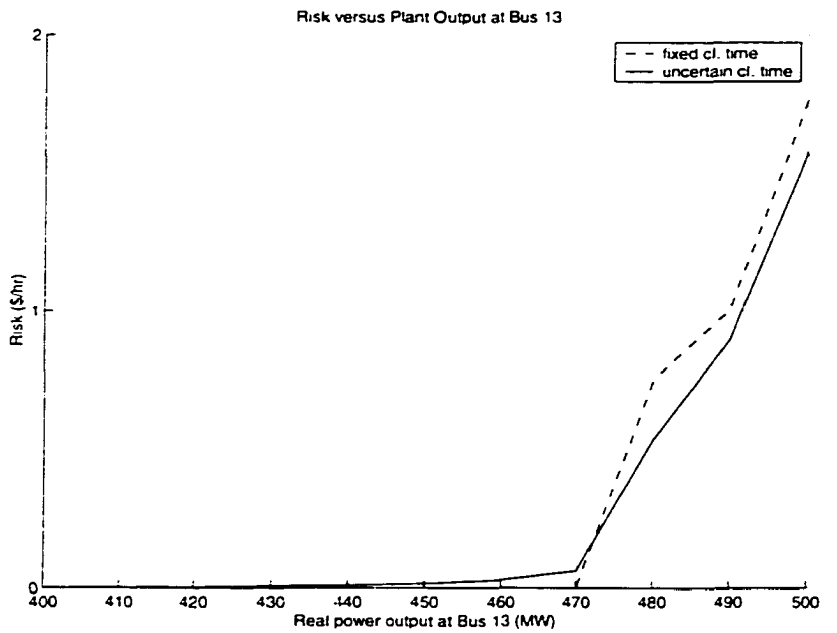

Figure 4-10. Influence of clearing time uncertainty on risk (zoom-in from the previous figure)

standard deviation of the total load. This plot provides an indication of how important or negligible this particular uncertainty really is. The dashed line corresponds to the original risk curve with the load level equal to the predicted load level. The solid lines are the -2σ and the +2σ risk curves respectively.

From Figure 4-11, it can be concluded that the 2% load uncertainty does not cause any significant impact on the risk calculations, since the %95 confidence interval is very narrow. Therefore, the load can be considered known for a one-hour ahead risk evaluation procedure.

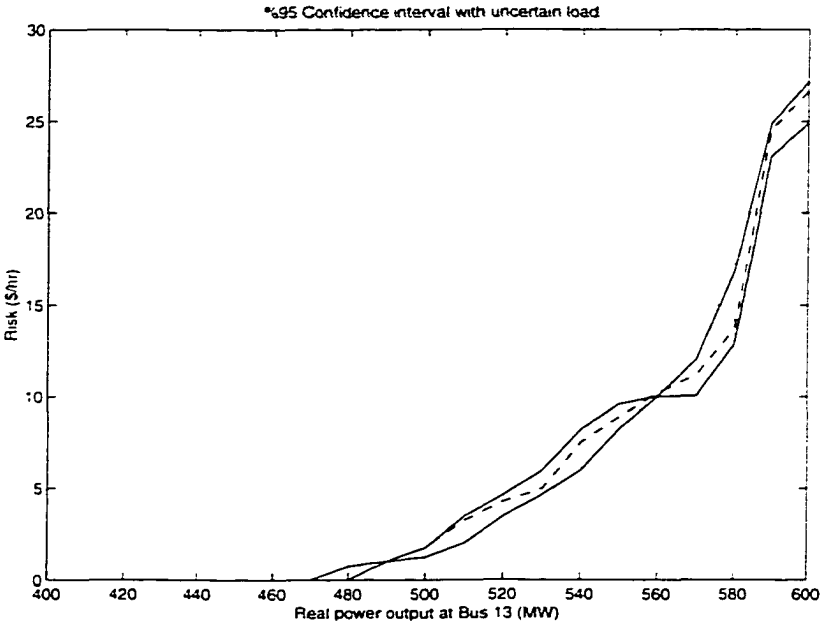

Figure 4-11. 95% confidence interval with uncertain load

4.5 *Influence of operating parameters on Transient Instability Risk*

In this section, risk is computed for variation in specific operating conditions within a range. The goals are to illustrate how the risk might be usefully portrayed to an operator and to establish that the risk variation reflects variation in system stress levels. The uncertainties that have been modeled are: fault rate, fault type, fault location and fault clearing time.

4.5.1 Local load

A local load is connected at bus 13, which is also the bus with the plant at-risk. The load is increased while all other parameters are kept constant, except the generation at Bus 21 which is used to compensate for the change of load. As Figure 4-12 shows, risk decreases as the load at Bus 13 is increased.

For a given generation level at Bus 13, a part of this power will be used to supply this local load. The rest will flow to the system. If the load increases, a larger share of the generation will be used to supply the local load, and less will be sent to the lines, i.e., the lines will be less loaded. As a result, the faulted lines will be off-loaded when the indicated load and compensating generation increases. It is observed that the rotor angle in the case of the larger load value is actually smaller than in the case of a smaller local load value. As a result, the generator will easierly go unstable when local load is small, and vice versa.

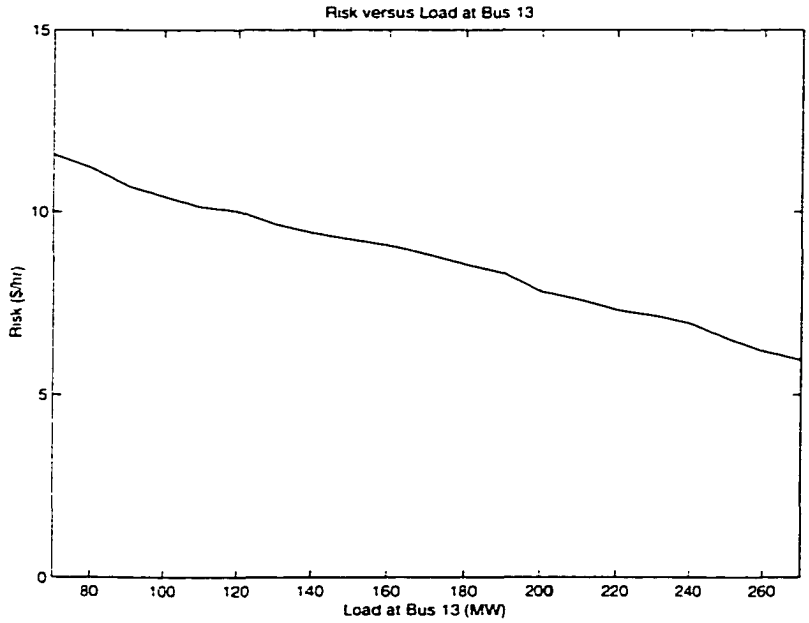

Figure 4-12. Local load level.

4.5.2 Total load and total generation

The next plot is to illustrate the effect of the dispatch policy on the risk of transient instability. In Figure 4-2, the dispatch policy was to compensate the change in the plant output by a change at generator 21. Now, in this case, (Figure 4-13) the total system load is changing uniformly, compensated by a uniform change of all generator outputs throughout the system[5]. It can be seen that both plots are very similar, indicating that the dispatch does not have a significant influence on the risk value.

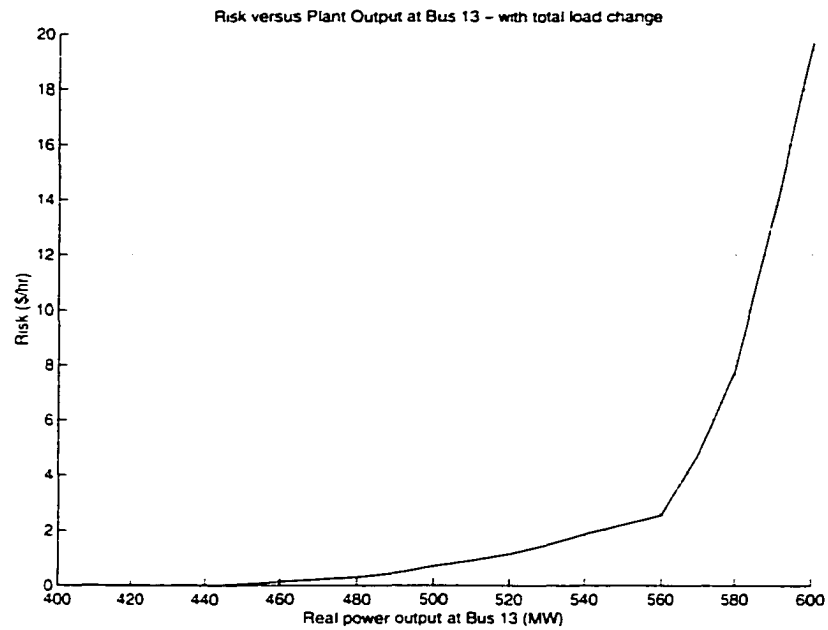

Figure 4-13. Proportional total load and total generation variation

4.5.3 Voltage level generator terminals

When changing the voltage set point of the generator, Figure 4-14 shows that the risk for instability decreases as the terminal voltage increases. This is understandable since with lower voltage levels, the accelerating power is smaller, and therefore, the chance for instability increases.

[5] The changes in load and generator level are done through a multiplication factor.

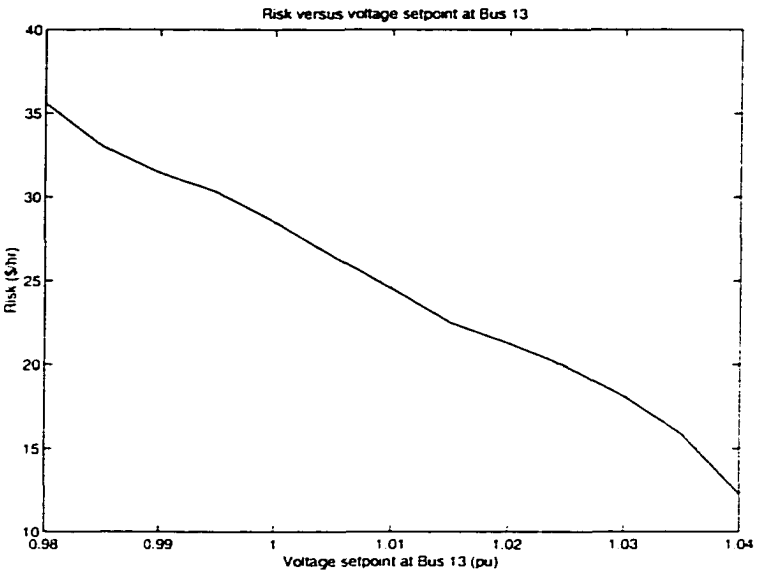

Figure 4-14. voltage level generator terminals

4.5.4 Generation level neighboring plant

Here, the effect of the generation of a neighboring (30 mi) plant power output is investigated (Figure 4-15). As expected, the influence is much smaller than in the previous case, but it is still perceptible.

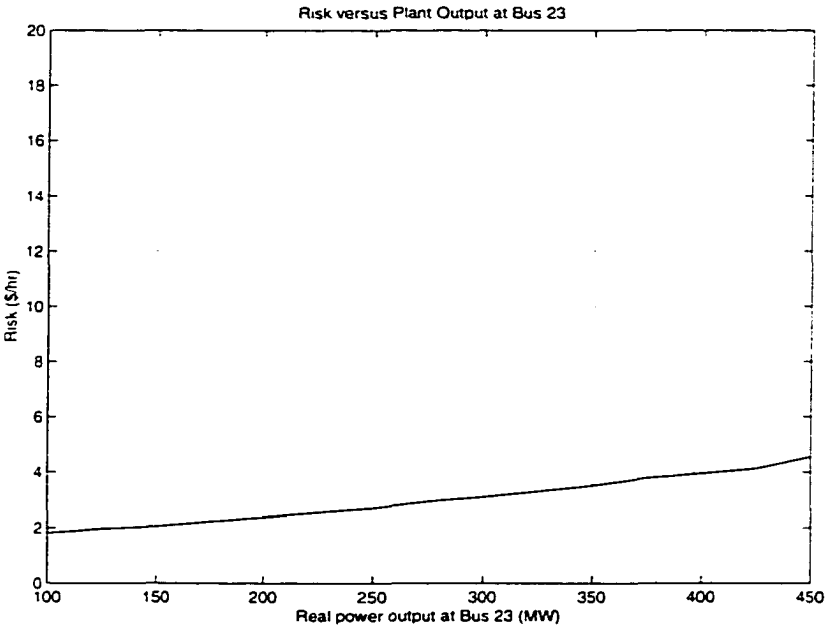

Figure 4-15. Generator level neighboring unit.

4.6 Summary of the chapter

The objective of this chapter is to give results of transient instability risk calculations obtained on a test system. First, it is tested whether the uncertainties of parameters discussed in the chapter 3 really have an influence on the risk calculation. The results show that the fault clearing time error should not be neglected since it has a significant effect on the stability. The one-hour ahead pre-fault load level prediction error, however, is not relevant in the risk calculations. The rest of the chapter is dedicated to visualize the effect of some other parameters on the risk. In particular, the generation level of the plant at risk is a crucial factor. It also demonstrated with the risk approach, that the deterministic operating limits do not correspond to risk level equal to zero.

5. FAST RISK ASSESSMENT

In order to have a tool that can be useful and practical in an operation environment, it should meet the minimum performance requirements in terms of speed and accuracy. In fact these requirements are in direct conflict with each other. In a planning environment, high accuracy is a higher priority than speed: there is not really a pressure to get a rapid answer.

In an operation environment, however, speed is probably at least as important as the accuracy. In a pre-contingency selection, where a large number of contingencies are screened, speed is favored over accuracy. Later, with the subset of 'dangerous' contingencies, the assessment is repeated, but this time with higher accuracy.

In order to evaluate the risk of transient instability in an operation environment, the assessment procedure must be fast. In the risk assessment procedure developed in section 3.3.2, the number of transient stability assessments to be performed can become very large. For example, when two lines are found to be critical, with these lines divided into 10 segments, and 4 fault types are considered, the risk value of one operating point requires 2x10x4 = 80 stability assessments. In chapter 2, an index was presented to measure numerically the level of transient stability. This index allows automating the complete simulation procedure. Still, the number of simulations to perform remains the same. The problem gets even more serious when risk-based nomograms introduced in chapter 1 are considered; in order to obtain a sufficiently high accuracy the number of operating points in the nomogram for which the risk is calculated should be at least 150. At 80 stability assessments per operating point, the number of the number of stability assessments can exceed 12,000 for single nomograms. To have these risk-based nomograms updated several times during the day, it is essential to find efficient ways to calculate the risk.

This chapter is dedicated to suggesting ways to reduce the number of time domain simulations to perform, or to propose alternatives to these simulations. In section 5.2, several rules are discussed to decrease the number of redundant simulations. Section 5.3 proposes an alternative to the time consuming simulations by using artificial intelligent techniques, with special emphasis on Artificial Neural Networks (ANN). Finally, section 5.4 provides an overview of all possible speed enhancements.

5.1 Reducing the number of transient stability assessments

5.1.1 Predictable cases

A large number of transient stability assessments (TSI calculations) can be avoided when making the following two assumptions:

1. When the system remains stable after a three-phase fault at the terminals with clearing of a single line (worst case), faults of other types and on locations further away from the generator will be stable. Faults on that line will not contribute to any risk.
2. When a single-phase fault at the far end of a circuit (opposite to the generator bus, i.e., best case), results in instability, any other fault at any other location will also result in instability. Again, no other assessments are needed. Faults on that line contribute highly to risk.

In some cases, one or both assumptions made above are not valid. It has been shown in [45] that in some occasions, the stability may worsen with increasing distance from the generator terminals. According to the author, the capability of the exciter to enhance the stability behavior degrades as the fault is moved further from the generator. This is particularly true when the generator employs a fast, high initial response exciter.

In any case, these assumptions should be carefully checked before applying them.

5.1.2 Location search algorithm

If a fault of a specific type, applied at two ends of one line returns different signs for the transient stability index, a binary search algorithm can be used to find what the percentage is of the line where faults can cause instability. If the signs are equal, no other assessments are required and another type of fault can be applied.

This kind of reasoning, when valid, is likely to avoid a large number of unnecessary stability assessments.

This speed improvement technique, as well as the previous one, can only be used if only the sign of the stability index is of interest. As explained in chapters 3 and 4, if the fault clearing time is included in the model as a random variable, also the magnitude of the stability index is required.

5.1.3 Screening of faulted lines

The number of lines on which a fault can cause any machine to go out-of-step is usually limited. Therefore, an off-line screening is necessary to filter out those lines that do not cause any trouble even under very stressed conditions. Some well-established methodologies could be used for this purpose [55]. In the test system used, only two relevant lines were observed. This screening should be repeated for different topologies.

5.2 Use of Neural Network in Transient Stability Assessment

As explained in the above sections, the time consuming part of the algorithm is the transient stability assessment. This assessment can be characterized as a non-linear mapping from a large input vector (pre-fault operating state and fault conditions) to a single output value (the transient stability index). An alternative to the slow time domain simulations is the use of artificial intelligence to predict the TSI from the input vector. In this section, it is shown that this task can be done by artificial neural networks (ANN). Reference [56]

provides more details about the concept of ANN, while reference [57] discusses neural network applications in power systems.

In a very general way, ANN can be defined as a highly interconnected array of nodes, similar to the neuron structure in a human brain. The nodes (or neurons) have an activation function and are organized in different layers. The input vector is fed into the input layer, and the output is obtained at the output layer, with possibly several hidden layers in between. The neurons of the different layers are connected through weights. With the traditional back propagation algorithm, the training of an ANN consists in finding the weights by feeding it one by one, a large number of input vectors with an associated output and back propagating the error made by the ANN on the output.

5.2.1 Literature

The combination of artificial intelligence (AI) techniques and power system security assessment is far from new. Techniques that had been used in signal and image processing made their entrance in the world of power systems some 30 years ago. It became clear that tools were needed to rapidly identify the operating limits in order to avoid operating in the insecure, and to allow operating closer to the boundary resulting in more efficient use of the available generation and transmission infrastructure. The main challenge was and still is to reconcile two inherently adverse aspects of the assessment; the speed and the accuracy. The primary objective has been to use these fast assessment techniques to filter quickly a large number of contingencies that pose no stability problems. The few remaining contingencies could be analyzed in more detail using the slower, but more accurate time domain simulation.

Pattern recognition (PR) was the first AI method to be applied to dynamic security assessment. In reference [58] Pang et al. suggested the use of PR for classification purposes. A pattern classifier is trained off-line using the results obtained from time domain simulation. The objective is to quickly classify an operating state as transiently 'stable' or 'unstable'.

Reference [59] was a milestone in the use of AI in dynamic security assessment: in this paper, Sobajic and Pao suggested the use of ANN to predict the critical clearing time from a reduced input vector including information about the fault location, pre-fault

operating point, and protective relaying strategy. Since then, a large variety of ANN applications in dynamic security assessment has emerged. Many of them include small improvements with respect to reference [59] or combine ANN with other techniques [60]-[62]. An overview of ANN applications in dynamic security assessment (DSA) is given in [63], where also the capabilities and limitations of ANN in DSA are discussed.

The use of rule-based expert systems for this purpose has also been proposed. The major weakness of this method is the fact that they are very case dependent, or in other words, their ability to generalize is very limited [64]. Decision trees are usually labeled as an AI method applied to can also be applied to fast transient stability assessment but is also often categorized as a special type of expert system. Here decision rules are provided by an inductive inference method. While the success of the decision trees has been demonstrated in different papers, it has not sparked as much interest as the ANN method.

Some authors have been suggesting the combination of different AI techniques in order to develop a method bundling the good features of the individual techniques. In reference [66], Song et al. combine pattern recognition with neural networks for transient stability assessment. Another example of this is given in reference [67] where Peças Lopes et al. use kernel regression trees, consisting of a combination of kernel regressors and decision trees.

The reasons why ANNs are very popular in fast transient or dynamic security assessment applications are:

- Prediction of performance index values (stability margin, transient stability index, critical clearing time, frequency deviation, etc.) by ANN is very fast,
- As a non-linear mapping tool, ANN has excellent generalization capabilities,
- The sensitivity of the TSI with respect to the input vector can be estimated directly from the weights.
- By keeping a knowledge base, using previous operating points, the ANN can be easily updated.

For the needs of the work described in this dissertation, ANN were selected to map the pre-fault operating conditions into the transient stability index presented in chapter 2. In

addition to the aforementioned reasons, it should be said that a trained neural network can also easily be integrated in the risk calculation software. It was not in the scope of this research to investigate very deeply all-possible AI techniques that could be applied to this problem, but simply to show that one of the most common applied techniques, the ANN, improves significantly the speed characteristics of the risk calculation procedure presented in chapter 3, making it useable in a operation environment.

5.3 Creating an ANN to predict the transient stability index

The creation of a neural network comprises several stages that are explained in this section. The stages are:

- Training and test set generation
- Feature selection
- Training and test process

5.3.1 Training and test set generation

In fact, this is an important stage independently of which artificial intelligence technique is being used. Ultimately, the neural network performance depends totally on the information that is contained in the data set. Therefore, it is crucial that the set has the following characteristics:

- High resolution
- Good distribution
- Sufficient breadth of information

A software tool was developed called "automated transient stability assessment software" or ATSAS to create large data sets with the above-mentioned characteristics in an automated fashion, not requiring the intervention of the analyst. It produces data files or data sets with a large number of samples. All samples of each file correspond to different pre-fault operating points to which the same type of fault is applied and on one of the circuits. The

data are built such that each row corresponds to a sample or an operating point described by the values of the operating variables together with the resulting transient stability index, obtained through simulation.

ANNs are known to be excellent in non-linear interpolation but have a worse performance in extrapolation. Therefore, it is important to generate data that captures the breadth of the complete feasible operating range. Attempts to use the neural network outside this operating range will result in diminished accuracy.

In the next two subsections (5.3.1.1 and 5.3.1.2) it is explained how to obtain the desired characteristics of the training set mentioned earlier. First, it is necessary to classify certain pre-contingency operating parameters according to different groups.

5.3.1.1 Critical pre-contingency parameters (CPPs)

Some pre-contingency operating parameters are expected to be good predictors of the performance measure. This is equivalent to saying that they are expected to be influential with respect to the transient stability behavior of the system. They can be any operating parameter that can be monitored in the control room and are typically selected through experience and by physical understanding of the security problem. The engineer should overselect in choosing the CPPs; if there is a doubt about whether a parameter should be a CPP or not, then it should be included as a CPP.

Another sub classification is made by distinguishing *independent* from *dependent* CPPs. Independent CPPs are typically inputs of the power flow calculation (active generation levels, voltage setpoints, load level, etc.) while dependent CPPs are the results of a power flow calculation.

5.3.1.2 Sample generation

Next, the samples are created according to a systematic procedure. From the set of independent CPPs, a small subset is chosen of CPPs with the highest expected influence on the stability response of the system. The parameters included in this subset are designated as the Monte Carlo CPPs (MCPPs) for reasons that will become clear later. The number of MCPPs defines the dimensions of the hyperspace from where the samples will be taken.

The complete operating range of each one of the MCPPs is divided into equal-sized intervals. Consequently, the hyperspace can be seen as being divided into smaller hypercells

having dimension corresponding to the length of the intervals. The sampling procedure consists of a step-by-step advancement through the hyperspace, and a sample data point is obtained for each hypercell.

The next step is to decide where in each cell to sample. One simple approach would be to sample the center of each hypercell or a specific corner of the cell. A two-dimensional example is shown in Figure 5-1. This approach guarantees a uniform distribution of sampled data points, but not necessarily a high resolution.

An alternative way to sample is presented in Figure 5-2. Instead of taking fixed points in each cell, a sample data point is chosen randomly within each cell. This method, referred to in this work as Monte Carlo sampling, leads to a highly resolved data set, because many different values of the parameters will be present in the set. This approach is motivated by the assumption that neural network accuracy, for a given number of data sample points, is best when each parameter is maximally resolved. In the literature, this method is also referred to as the *latin hypercube sampling* [69, pp. 553-555].

After the selection of the MCPPs, the values of the other CPPs need to be assigned their values at each sample data point. Depending on the nature of the parameter, this value can be chosen randomly over the operating range of this parameter.

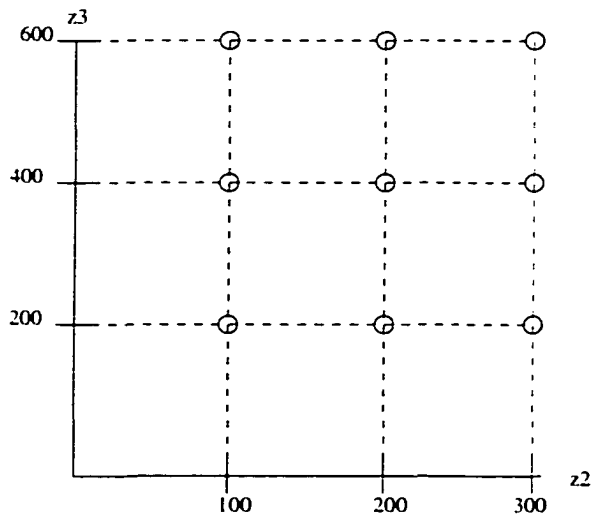

Figure 5-1. Structured sampling in two dimensions.

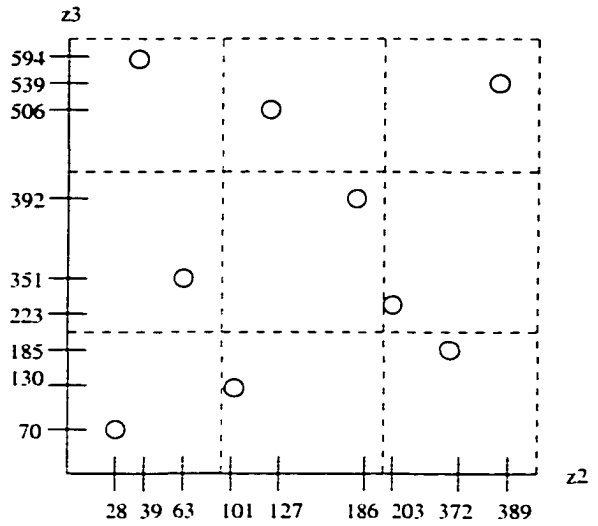

Figure 5-2. Monte Carlo sampling in two dimensions

Once the values for all CPPs are specified in a hypercell, the simulation is performed, starting with a power flow solution to determine the pre-fault operating conditions, followed by a time domain simulation and stability index calculation. Finally, the parameter values and the index are stored in the data file and the procedure advances to a new hypercube.

This method guarantees a good distribution and high resolution, if the number of segments is high enough. As mentioned before, to obtain enough breadth of the information contained in the data set, the operating values of the parameters should cover the complete feasible range. The complete sample generation algorithm is presented in Figure 5-3 and is based on the method described [70].

The software that has been developed to create the data set, monitors the input and the output of several simulation routines, (power flow calculation and the transient stability assessment) and performs the transient stability index calculation.

Before starting the data generation program it is also necessary to consider the time allocated for this generation procedure. The required generation time depends directly on the number of hypercells in which the hyperspace has been divided. Therefore, to obtain a data set with a good enough accuracy within a reasonable amount of time, a higher number of intervals should be chosen for MCPPs with an expected important influence on the post-fault

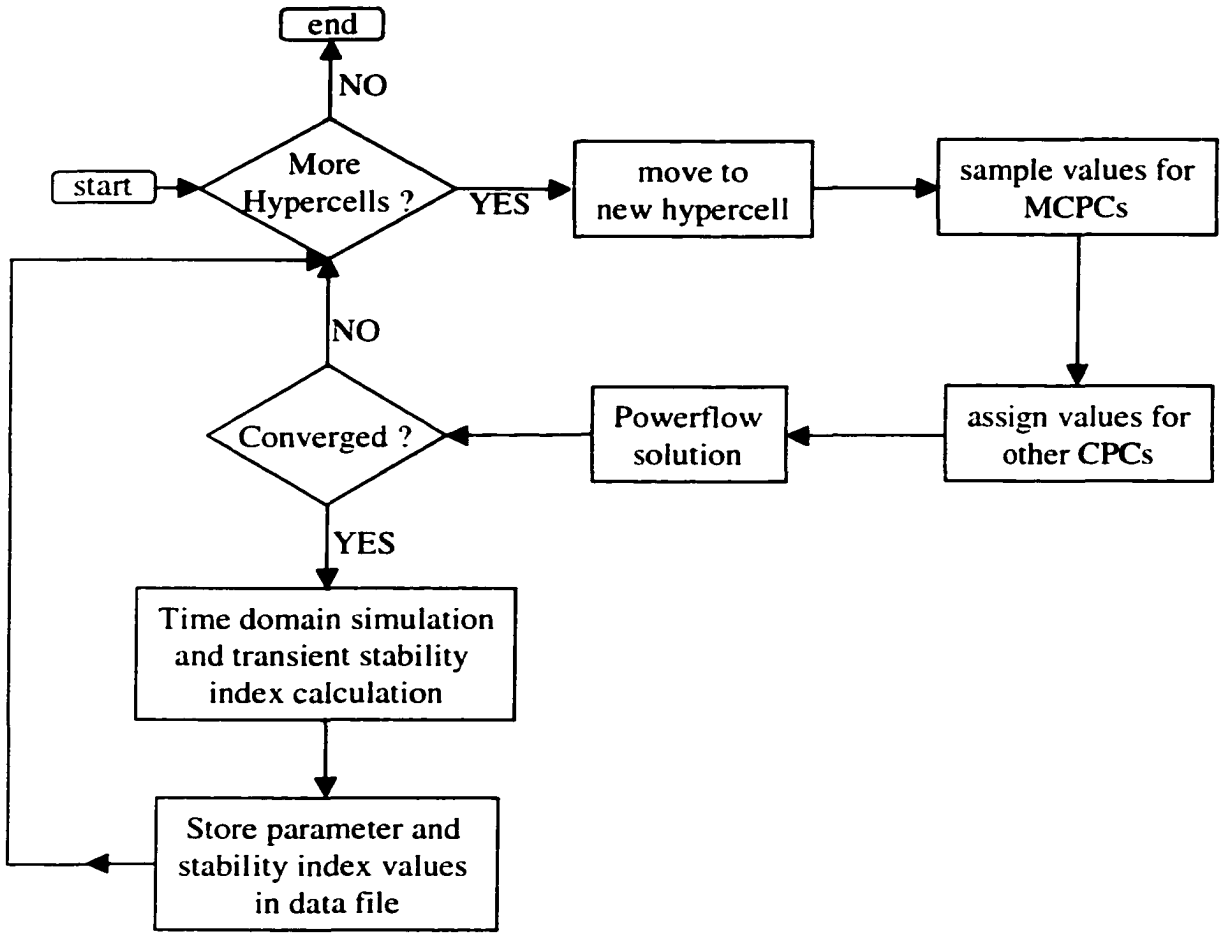

Figure 5-3. Automated transient stability assessment.

system behavior. In addition, the number of MCPPs should be limited depending on the speed of the available computer.

5.3.2 Feature selection

As was mentioned in 5.3.1, the objective is to overselect the parameters characterizing a sample data point in order to ensure no relevant information is missing in the final data set. Ultimately, this parameter or feature set will be used as an input to an ANN, and the output will be the transient stability index, using the data in the file to train and test the ANN. On the other hand, an excessively large set of features might have some drawbacks:

- The larger the feature set, the slower the ANN learning process,
- Some of the features are hardly or not relevant and will introduce some noise in the information, which will diminish the accuracy,
- More samples are needed if the feature set is large, in order to obtain a sufficiently accurate ANN.

For these reasons, it is necessary to find a smaller subset of features that does not contain redundant information and that performs best in predicting the ANN output. This subsection describes an approach to automatically select the most critical parameters or features. It is important to mention here, that this selection is not meant to replace the engineering judgment, but to confirm it and to complement it by giving additional information.

In this work, a genetic algorithm is used to search the possible combinations of features and to come up with a list of subsets that perform well as neural network inputs. A neural net-based genetic algorithm was used to select this subset of features. Only the major points of this technique will be discussed in this work, more details can be found in [71].

5.3.2.1 Genetic algorithms (GAs)

A good definition of what genetic algorithms are can be found in reference [73] where the author states: "Genetic algorithms are search algorithms based on the mechanics of natural selection and natural genetics". GAs are especially useful to search for solutions in combinatorial problems with discrete solutions for which a performance measure (a.k.a. fitness) can be defined for each solution.

The GA process works as follows: an initial population (or group) of binary bit strings is created randomly. This is also called the first generation. Each string of ones and zeros corresponds to one solution. Depending of the application, the binary coding of the solution can have very different meanings. To evaluate the worth of each solution according to the criteria of the problem, a fitness function needs to be defined that will return the "fitness" of each solution.

In order to evolve to the next generation, the population needs to undergo several operations: reproduction, crossover, and mutation. Many variations of these operations have

been developed. In the reproduction phase, the fitness is used to measure the ability of a solution to survive and to be present in the next generation. Crossover and mutation consists in trying to introduce new genetic material in the population, with the hope that newer and better solutions, i.e. with better fitness, will emerge.

The algorithm continues to evolve through a large number of generations until the population does not improve anymore.

5.3.2.2 GA application to feature selection

An exhaustive search for the optimal subset of features to be used as an input for a ANN to predict the transient stability index is generally not feasible due the usually high number of pre-selected features[6]. As mentioned before, in this work, GAs are used to determine a selection of quasi optimal subsets. The idea to use genetic algorithms for feature selection has been suggested, among others by Vafaie et al. in [72]. The software package GANN, developed at Iowa State University, was used for this purpose.

In this application, each solution is represented by a binary vector consisting of a number of bits equal to the number of pre-selected features. Each position in the string corresponds to a feature or attribute. A '1' on a certain position means that that feature will be used as an input feature, while a '0' indicates that it will not be used. To compare the solutions or the individuals of the population it is necessary to evaluate their performance; a fitness function has to be defined. The fitness function used in GANN combines two aspects, accuracy and cardinality. The total fitness F is given by equation 5-1.

$$F = w_1 F_1 + w_2 F \tag{5-1}$$

- Accuracy fitness F_1

  A small neural network is trained using the inputs corresponding to the selected features of the individual. Accuracy fitness is measured by the reciprocal of the average absolute error computed by testing the neural network.

---

[6] With 30 pre-selected features, then number of combinations will be 2^{30}=1,073,741,824

- Cardinality fitness F_2

  Cardinality is the number of features that are selected in the individual, i.e., it is the number of '1's present in the solution. A desired number of cardinality is specified and if a solution contains more selected features than the desired cardinality, the cardinality fitness will be zero. Otherwise, F_2 will be equal to the number of features present in the solution.

The weight w_2 is usually very large compared to w_1. The Multi-layer Back propagation neural network is used because of its computational efficiency and its ability to perform nonlinear functional approximation. In order to limit computation time, a simple neural network structure with only one neuron in one hidden layer is used. In this work it is assumed that the feature set that performs best with this simple structure will be at least one of the best for more complicated structures.

5.3.3 *Training & testing of Neural Network*

After obtaining the satisfactory subset of critical pre-contingency operating parameters, a neural network is trained with this subset as input to predict the transient stability index. The multi-layer back propagation neural network model is used. The data set is divided into a training and a test set. The test set is not used to train the ANN but is fed into the trained ANN to evaluate its generalization capabilities.

It still has to be specified which ANN architecture to be adopted. Several heuristic methods have been suggested in the literature. As a general rule it can be said that if the structure is too simple the training error will be large. The training error is the error of the ANN when using the data samples of the training set only. If the structure is too complicated the learning error will be small enough but the generalization capabilities will be limited, resulting in large test errors. The 'optimal' structure can be found through trial and error.

Instead of the traditional back propagation algorithm with fixed and unique learning rate, an adaptive back propagation is used, with an individual adaptive learning rate for each weight. The learning process with this algorithm is much faster [61].

Once the ANN has been trained, the ANN is implemented in the risk calculation module by rebuilding it according to the optimal architecture and the obtained weights.

This work does not claim to employ the most advanced NN technology. Many newer, and probably more efficient algorithms have been developed in the recent years. The only objective of this chapter is to show that even with a 'conventional' ANN it is possible to considerably speeding up the risk calculation process by predicting the transient stability index from the pre-fault operating conditions.

5.4 Illustration

As explained in chapter 1, many utilities operate their system with the help of a set of nomograms to indicate them the deterministic operating limits in the space of 2 critical operating parameters. As an alternative to these deterministic limits, it is proposed to plot in the same space, the contours of equal risk. In order to do this with a sufficient accuracy, the risk value of a large number of points needs to be computed. The contours will be drawn by interpolating through these points.

The computational intensity of the risk calculation has been identified in this work as a difficulty. This problem is even more severe when considering risk-based nomograms. The nomograms should be updated ideally every 15 or 30 min. It is for this application that artificial neural networks are very useful, as will be shown in this section.

The objective is to draw contours for the previously presented case taken from the IEEE RTS system, where faults on two lines leaving bus 13 can cause transient instability at the plant at Bus 13. The two critical parameters selected for the abscissa and ordinate of the nomogram are the *load level* and *the generation level at bus 13*, respectively. It is estimated that the risk value of approximately 200 operating points in the space of these two parameters needs to be calculated in order to obtain a graph with sufficient accuracy.

The problem was approached the following way: the two lines and the 4 fault types correspond to 8 different events, because they are really distinct phenomena. As a result, eight data sets were created, one for each event. These eight data sets are then used to train

and test eight different neural networks predicting the stability index. When the training and testing phases are completed the ANN are incorporated into the risk calculation software.

Learning and test set

Using the software described above, eight data sets were created with over 5.000 samples each.

Feature selection

After running the GANN software and using engineering judgment, the 12 attributes were selected to represent the input of the neural network, as listed in Table 5-1.

Table 5-1. Selected features for ANN training

Selected Features
Individual active power levels of the 3 units at Bus 13*
Total active power level at Bus 23
Total active power level at Bus 23
Load at Bus 13
Active power level unit 2 at Bus 15
Active power level unit 2 at Bus 2
Active power level unit 3 at Bus 1
Flow through faulted line
System power factor
Fault location (number of segment on faulted line)

*This is to indicate which units or 'on' or 'off'. The units of one plant that are operating are assumed to have the same generation level.

Due to the high number of samples, the GANN feature selection process was very slow. One of the possible problems that can occur while using GAs, is that the algorithm can be stuck in a local minimum. To avoid this, several GA runs were performed each team with different settings for the GA parameters (initial population size, mutation and crossover probability, etc.). From each one of these runs the top 20 best solutions were extracted for closer evaluation and comparison with solutions from other runs.

Training and testing

The data sets are randomly divided into training sets (70% of the samples) and test sets (30%). After several trials, in most cases the best architecture was found to be one with 2

hidden layers: with 10 and 8 hidden neurons, respectively and in one case, 8 and 6 neurons, respectively. Again, due to the large number of samples, the training process was rather slow.

5.4.1.1 Visualization of contours of equal risk

In order to plot these contours, the risk value of 200 points in a grid in the diagram is calculated. First, the exact risk values are calculated by determining the transient stability index through time domain simulation. These calculations provide a reference will to compare the accuracy of the neural network. The contours using those reference calculations are displayed in Figure 5-4. These plots are computationally intensive to obtain because the dependent CPPs require updating each time the independent CPPs are changed.

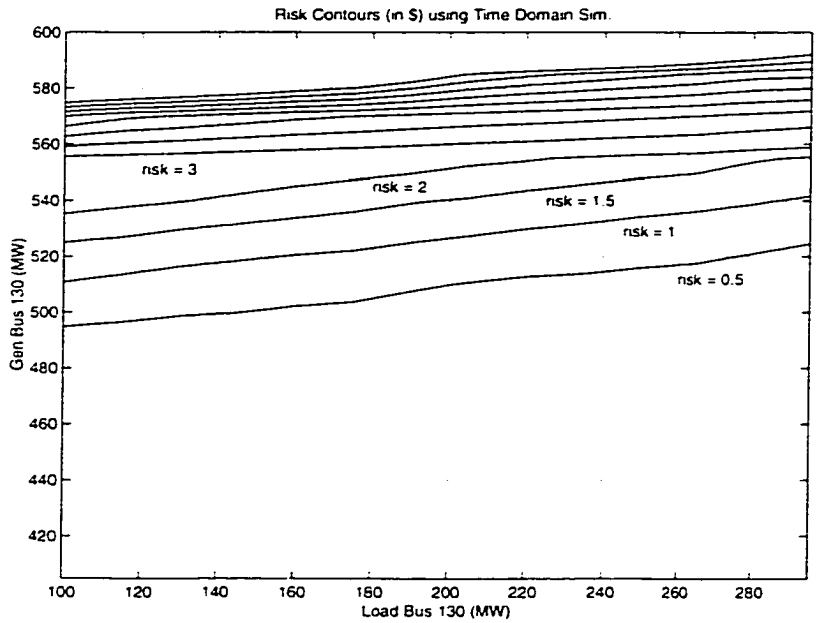

Figure 5-4. Risk-based nomograms obtained with time domain simulation

The same graphs are plotted in Figure 5-5, but this time with the eight trained neural networks. The speed gain obtained is impressive. While Figure 5-4 is obtained in approximately 18 hours on a 125MHz, 64Mb RAM processor. Figure 5-5 only takes about 45 minutes. The accuracy of the risk values obtained with ANN is about 1.8 $/hr in average. It is observed that the accuracy is higher for larger risk values than for smaller ones. This might have to do with the fact that the learning sets did not have sufficient low risk points. the

These results could further be improved by investigating on the other possible architectures, and applying more sophisticated feature selection algorithms. When the selected neural network inputs are all independent variables (loads, generation, voltage set points, etc.), the nomogram is plotted in only a few minutes, but at the cost of an even lower accuracy. The speed enhancement here is achieved because the updating of the dependent CPPs is avoided.

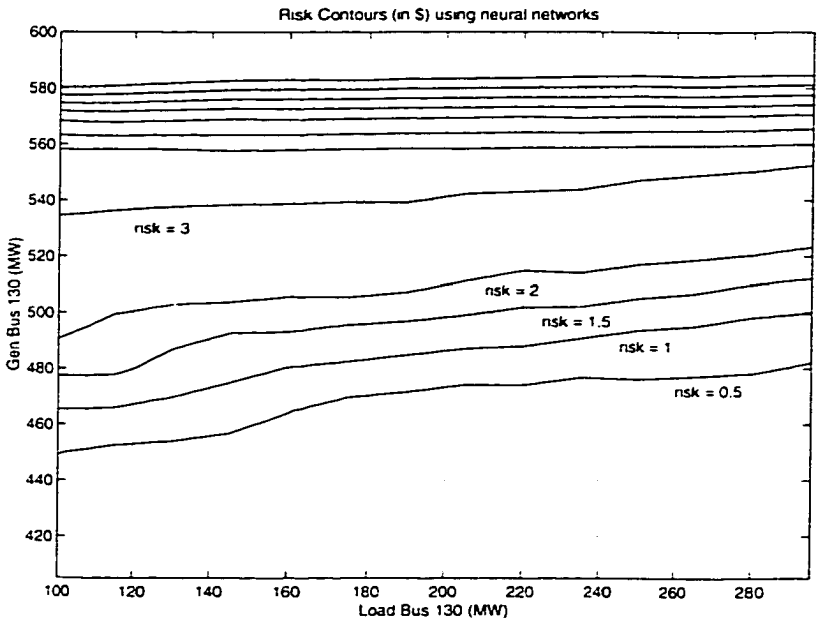

Figure 5-5. Risk-based nomograms obtained with ANN.

5.5 Overview of possible ways to improve speed of risk calculation

The following table presents an overview of the different techniques available to reduce to computational effort of the risk calculation procedure. If all these techniques were applied to it, the procedure and the plotting of risk-based nomogram plotting is expected to be feasible in an on-line environment.

Table 5-2. Overview speed improvement techniques

Method	*How is time reduced*	*Description*	*Implemented?*
Predictable cases	eliminates unnecessary stability assessments	In some cases sign of stability index can be predicted from previous stability assessments	YES
location search	eliminates unnecessary stability assessments	Fraction of the line is determined where a specific fault causes no trouble	YES
screening of faulted lines	eliminates unnecessary stability assessments	Eliminates lines where faults will cause no trouble	YES
Early termination	reduces the simulation time	As soon as the transient (in)stability is detected the simulation is interrupted	YES
artificial intelligence	Fast AI prediction instead of stability assessments	Use of ANN to predict stability index from operating conditions	YES
parallel programming	simultaneous stability assessments	Parallel processing can be done by fault type, fault location, or by dividing the range of the nomogram parameters	NO

5.6 Summary of the chapter

In this chapter special attention was given to the problem of relieving the computational effort inherent to the risk calculation. Several rules are suggested to diminish the number of time domain simulations to perform.

In addition, it is proposed to use artificial neural networks as an alternative for the time domain simulations. The neural network can be trained to predict the transient stability index. After discussing the several phases of the neural network training, including training set generation, feature selection, and the actual neural net training, the usefulness of this approach is illustrated with the plotting of risk-based nomograms. It is shown that the use of neural networks provides significant time gains when used to predict the stability index instead of calculating the index from time domain simulations.

6. RISK-BASED DECISION MAKING

In the previous chapters, the focus was on developing a methodology to calculate risk of transient instability, particularly how it can be derived and how the associated computational intensive procedure can be alleviated. In addition, different ways to visualize the risk were presented.

So far, little was said about how this risk measure can be used. The merit of a security index can be even more emphasized, if its usefulness in different applications can be shown. In this chapter, it is shown how risk can be used in an operation decision-making framework, where risk is one of the attributes of the decision problem. Although the discussion is confined to risk of transient instability, it is generally applicable to other security problems as well such as overload and voltage insecurity [10][11][13].

6.1 Problem description

On many occasions, an engineer faces the problem of having to make decisions of various kinds with various levels of possible consequences. The use of a rational decision aid tool is most important when the decision-maker is under psychological stress due to time constraints, situational complexity, and high cost consequences for poor decisions. Such a tool uses as much as possible the available information to help the engineer make the 'best' decision, or at least the most defendable. Power system planning engineers deal with decision-making problems, such as having to select a specific type of new equipment, the location of new substations, choosing possible expansion projects, etc.

In system operation the decisions need to be made in a very short amount of time (maximum a few hours). The problems can be complex too, and the consequences of a wrong

decision can be felt immediately. Usually, the number of alternatives available to the system operator is limited. As a result, decision aid tools are also very helpful in an operation environment. The thrust of this chapter is to pose the decision problem faced by the operators and to report on investigations into various solution approaches. Some necessary terminology is defined in the next section to begin this discussion.

6.2 General model of a decision problem

A decision-making problem has generally the following components:

- *Criteria*: higher-level, sometimes abstract goals, like for example, maximizing community welfare, or minimizing criminality, or maximizing customer satisfaction. A problem can have different criteria, often one conflicting with another, resulting in a multiple criteria decision-making problem.
- *Decision maker (DM)*: this can be one person or a group of people who have the responsibility and the authority to make the decision.
- *Alternatives*: a certain number of choices are available to the decision maker, called alternatives, actions, or options. If the number is infinite or uncountable, then the problem is an optimization problem, which is a specific type of decision problem that is not covered in this chapter. The way these alternatives are created will not be discussed here either, and it is therefore assumed that the different alternatives have been specified previously and are known to the DM.
- *Attributes*: in order to evaluate the level of satisfaction of an alternative for a particular criterion, one or more measures are needed.
- *Objectives*: the objective is the direction (minimizing or maximizing) in which the DM wants to shift the value of an attribute. An objective is more specific than a criterion. A criterion can involve several objectives. For example, 'maximizing community welfare' is a criterion that includes several objectives. Community welfare can be measured by a number of attributes, such as unemployment rate, the number of green area acres, the number of people living on social welfare, etc.

The associated objectives correspond to minimizing or maximizing the value of the attributes.

- *Future scenarios or states of nature*: in many situations, the success (or failure) of the alternative depends on the future scenario. The attribute values of each one of the alternatives can be different depending on which scenario turns out to be true. If only one scenario can happen, the problem is called decision-making under *certainty*. With more than one scenario, the problem is defined as decision-making under *uncertainty*. In this case the likelihoods of the scenarios need to be specified by analyzing historical data or by the input of experts.

Though these definitions are found most frequently in the literature, they are not used universally. Nevertheless, they will be employed consistently throughout this work.

6.3 Study case

The decision maker (DM) is assumed to be in charge of the generator plant in a 3-bus subsystem or area of the IEEE reliability test system comprising Buses 12,13 and 23 (see 4.1), and he/she is in charge of selecting an operating action for the coming hours.

Table 6-1 presents the options available to the system operator, together with a qualitative description of each one of them in terms of security and profits. The DM's goals are mainly two-fold: to maximize the profits and to maximize the security.

In Table 6-2, the probabilities corresponding to each one of the relevant future scenarios are given. It may happen that no faults occur, or that either one of the two lines emerging from Bus 13 is faulted. Only the transient stability is considered, in this case. Other faults might also happen in the sub-system under study but do not affect the transient stability.

To measure the economic benefits of an alternative, the projected profits that result from that alternative are calculated. It is calculated as the difference between the revenues from energy sales and the direct production costs (fuel costs). These profits are shown in Table 6-3. This calculation is made assuming no fault occurs. The costs caused by a fault are

Table 6-1. Decision making case

	Description	*Security*	*Profits*
Action 1	Maintain present conditions.	Low	Medium
Action 2	Transfer 60 MW from bus 13 to bus 23	High	Medium
Action 3	Buy 150 MW from outside the area	High	Low
Action 4	Sell 130 MW to the outside	Low	High

Table 6-2. Probability of fault occurrence.

Scenarios		*Probability/hr*
Scenario 1	No outages	0.9999
Scenario 2	Line outage 13-12	4.58E-5
Scenario 3	Line outage 13-23	9.16E-5

Table 6-3. Profits.

	action 1	*action 2*	*action 3*	*action 4*
Profits($/hr)	20,385	19,902	10,602	22,595

Table 6-4. Security Cost.

$/hr	*action 1*	*action 2*	*action 3*	*action 4*
Scen. 1	0	0	0	0
Scen. 2	855,679	235,549	220,111	1,127,882
Scen. 3	671,221	133,461	133,461	671,221

accounted for in security costs (

Table 6-4). These costs differ for each action and under each scenario. They include, repair costs, load shedding cost, and opportunity costs [75]. Given this information, the task of the plant operator is to find out which one of the options, according to his/her experience and judgment, gives the best trade-off between economy and security.

6.4 Profits minus Risk – the single criterion case

If there is only one relevant criterion or if different criteria can be easily combined into one single criterion, the problem can be approached by single criterion decision-making methods. The differences among the various existing methods are related to the way the probabilities of the possible scenarios are perceived [76]-[78]. A possible criterion could be maximizing the difference between the attributes profits and security impacts. For each alternative under each scenario the resulting outcome (value of the attribute) is calculated. The best-known single criterion decision paradigms were applied to the presented problem and the results are summarized below. Additional description of this study can be found in chapter 11 of [9]. The first three paradigms are based on subjective assumptions on the scenario likelihoods, while the last two use probability data obtained from historical data or through calculation.

1. *Maximin paradigm:* This is a pessimistic rule. It assumes that whatever action is taken, the worst scenario for that action will happen. The alternative that has the 'best' worst outcome is selected. Under this rule, action 3 would be chosen.
2. *Minimax regret paradigm:* Here, the regret associated with one option is quantified as the difference in outcome of that option and the outcome of the option that would have been chosen, if the future were known. For each alternative, the maximum regret value is identified and the alternative with smallest maximum regret value is picked. According to this rule, action 2 would be selected.
3. *Equal likelihood paradigm:* This rule assumes that all scenarios have the same probability of happening: the alternative with the highest sum of outcomes is selected. This would result in the selection of action 2.
4. *Maximum expected monetary value:* The outcomes are multiplied by the probability of occurrence of each scenario and then the balance is made of the expected profit and the total expected cost. Finally the option with the largest of these differences is chosen. The probabilities of each scenario from Table 6-2 are used here. In this case this would be action 4.

5. *Maximizing Profits minus* Risk: Instead of looking at the security impacts in each scenario, a risk index can be calculated using the approaches developed in [9]-[13]. The risk values for each action are presented in Table 6-5. Here, we account for transient instability, assuming the overload and voltage instability risks are zero. The probability of the *instability event* is considered in this paradigm, which depends on scenario likelihood and the probability of instability given the scenario. The alternative with the highest difference between profits and risk is selected, i.e., action 4.

Table 6-5. Risk values.

	action 1	***action 2***	***action 3***	***action 4***
Risk($/hr)	9.3	2.12	2.06	10.44

6.5 Multi-criteria decision making

6.5.1 Shortcomings of single criterion risk-based approaches

From the results obtained in section 6.4, it is apparent that the methods that do not use probability data (methods 1-3) are quite conservative, i.e., they select those actions resulting in the safest or most secure scenarios. On the other hand, the methods that do use probability data (methods 4 and 5) are quite risky, i.e., they select those actions that result in the most dangerous scenarios. Intuitively it can be felt that a proper decision paradigm for power system operations should result in decisions between these two extremes. Such a decision paradigm is believed to be obtained via improving method 5. Specifically, with respect to method 5, solutions are sought that overcome the following weaknesses:

1. *Risk measure does not tell the whole story*

   The use of risk as single measure of the security level alone might be not enough. As indicated before, risk is the mean of the cost consequences (or expected impact) of an insecurity event. It is probable that two operating points with the same risk value

correspond to two totally different situations. One situation may lead to catastrophic consequences but with low probability. The other situation may have a high probability of occurrence, but the impact is low. Although they have the same risk value (expected impact), the operator is certainly not indifferent to these cases. Risk alone does not distinguish the preference of the operator between these two cases.

2. *Incommensurability of risk and profits*

   The values for the profits obtained with each alternative appear to be incommensurate with the values for risk. An increase of risk by $1 is not compensated by an increase of profit by $1. Since risk is the product of probability and impact, the sometimes-large impact is weighted by the very low occurrence probability of the insecurity events, resulting in a small risk value. Adhering to the alternatives suggested this way leads to exclusively profit driven operation of the system. In reality, plant operators have a more conservative attitude, and they do consider security aspects. The above-mentioned objective (maximizing profits minus risk) therefore does not reflect the operator's attitude and, thus, its use as such should not be recommended.

Several ways exist to distinguish the 2 cases mentioned in weakness no. 1. One of them is using higher order moments, like for example, the variance (V) or standard deviation (σ) of the impact (Eq. 6-1) [79]. It measures the deviation from the mean, and it is a good way to evaluate the uncertainty associated with an alternative. Minimizing the uncertainty is now a third criterion. From this point on, only the standard deviation (σ) will be used. Returning to the two cases mentioned in comment no. 1, they can now be distinguished, since the first case would have a very large σ, while the σ in the second case would be more limited. The values for the standard deviations for each option are presented in Table 6-6.

$$V(A_i) = Pr(K \mid A_i) \cdot Im^2(K \mid A_i) - (Pr(K \mid A_i) \cdot Im$$

$$\sigma(A_i) = \sqrt{V(A_i)} \qquad (6\text{-}1)$$

where A_i corresponds to action i.

Table 6-6. Standard deviation for each option.

	Action 1	*Action 2*	*Action 3*	*Action 4*
Profits ($/hr)	20,385	19,902	10,602	22,595
Risk or mean ($/hr)	9.29	2.12	2.06	10.44
Standard deviation ($/hr)	1,725	935	921	1,829

A first step to improve the objective 'maximizing Profits minus Risk', would be to include a term corresponding to the standard deviation to be minimized (with a minus sign), which is also expressed in the same monetary units. But now, the problem mentioned in comment no 2 still remains, i.e., the incommensurability of the attributes to be optimized, now including the standard deviation.

One way and the most common way to get around this problem would be using weight coefficients to give appropriate importance to each individual attribute (Eq. 6-2).

$$\text{Max } f(\bar{x}) = \alpha \cdot Profits(\bar{x}) - \beta \cdot Risk(\bar{x}) - \gamma \cdot \sigma(\bar{x}) \qquad (6\text{-}2)$$

The weights could be provided by the operator according to his priority with respect to profits, risk and σ and how he would feel about the trade-offs between them. However, this approach is inappropriate because the weights given like this are arbitrary: their values will highly depend on the state of mind of the operator at the time of the inquiry. Arbitrary weights will lead to inconsistent results.

Several alternatives exist to provide values for the weights in equation 2 in a more systematic and robust way. The key is to obtain additional information from the Decision Maker (DM) from which the weights can be extracted. One possible way of doing this is by asking the DM to determine several sets of attribute values for which he is indifferent [77].

Since the problem has three criteria now, it is only natural to apply multi-criteria decision-making methods. Several approaches exist to deal with decision-making problems with various objectives or criteria, i.e. Multi-Criteria Decision Making (MCDM).

Nevertheless, it is important to keep in mind that an alternative that optimizes all criteria is very unlikely to exist. In the following a summarized overview of existing approaches is presented, and one of them will be applied to the example presented in section 6.1.

6.6 Literature review on multi-criteria decision making

An intuitive way of dealing with multiple criteria has always been attributing weights to the criteria according to their importance in the eyes of the DM. In [80] this decision-making methodology is approached from an academic point of view. In the 60's and the 70's a lot of effort was spent on the development of the value and utility theory and its application to problems with multiple objectives through the use of multi-attribute utility functions [81][82]. A derivative from these methods came out in 1980, Analytical Hierarchy Process (AHP) [83], and was particularly suited for problems in which the criteria present a hierarchical structure. In the early 70's a new kind of approach emerged, the outranking methods, introducing a more subtle relation between alternatives, the outranking relation. Several different versions and adaptations appeared having many applications in Europe [84]-[88]. More recent developments of these methods can be found in [89].

The 80's brought a wide proliferation of methods with varying degrees of success. Therefore, a classification of the methods became necessary. A comprehensive survey of MCDM methods and applications is presented in [95] and [96]. A comparison of the results obtained with several methods applied to one problem is presented in [97]. Another excellent overview including more recent methods is presented in [98].

6.7 Overview

The most reliable measure for a method is the degree of confidence the DM has in the method. For relatively simple problems, the decision made with the aid of MCDM should be compared with the decision the DM would make without any assistance. By giving the DM many similar decision making cases and comparing the answer by different methods, the one

that best matches the DM's natural answers can be considered as a good candidate. Another way to select an appropriate method is to consider methods that have been successfully applied to similar problems. In [96], several questions are listed to help the user to evaluate different multiple criteria decision-making methods.

Most of the books dealing with MCDM make a succinct classification of the existing methods. Here, a more detailed classification is proposed. First, it is necessary to distinguish the characteristics of a decision-making problem. A problem can be characterized by single or multiple criteria, by having either a finite countable number of alternatives or an infinite number. Objective probability data can be used to make a decision or subjective probabilities can be assumed, or it might happen that no uncertainty is involved. The methods can also be distinguished by their outcome: some only return a complete ranking with or without ties, or just the best one, or others will return a structured set of alternatives. Table 6-7 provides a classification of the methods. The top of each column shows different groups of methods, and the rows indicate various characteristics. Any other method can be added in one of the existing columns or by creating a new column if it has a different mix of characteristics. Additional rows can be added to include more characteristics like e.g. the number of alternatives. For example, optimization algorithms would require an extra column with the indication of an *infinite* number of alternatives, single or multiple objectives, *no* use of probability data, and the outcome is an *individual solution* if existing.

Methods involving multiple criteria have the particularity that they do not and cannot provide an 'optimal solution'. The process to get a 'solution' – perhaps the term 'suggestion' would be more appropriate - is based on additional subjective information provided by the decision-maker characterizing his or her preference.

6.8 ELECTRE IV

In most MCDM methods, the outcome results in a ranking of the alternatives, with possible ties. However, in some situations, given the preferences of the DM, no distinction can be made between alternatives. In spite of this evidence that no distinction should be made, it appears that many methods are forcing this distinction by making overly strong

Table 6-7. Multicriteria decision making methods.

	Minimax, Maximin, Minimax regret	***Expected monetary value***	***Multi attribute utility function, AHP,MACBETH****	***Outranking methods***	***Fuzzy Sets and Rough Sets based methods***
Number of objectives	Single	single	multiple	multiple	multiple
Use of objective probability data	no	yes	yes/no	no	fuzzy/rough
Outcome of the method	rank	rank	rank	Structured set of alternatives	rank

*Measuring Attractiveness by a Categorical Based Evaluation TecHnique

assumptions on the preferences stated by the DM, and some methods cannot provide any solution at all. These cases are due to the requirement that each alternative should be comparable (preferred or equivalent) becomes restrictive. In the approach presented in this section, ELECTRE IV, this restriction is omitted. It allows declaring two alternatives incomparable with each other.

The first of a series of outranking methods called ELECTRE appeared in 1968, and after that several more developed and advanced versions came out [84]-[90]. In section 6.9, the ELECTRE IV method will be applied to the decision-making case presented in section 6.1. Each step of the method will be explained in detail.

6.8.1 Principles of the ELECTRE IV method

From all the existing methods, ultimately the basic version of the ELECTRE IV method was chosen, which is based on the outranking principle [98]. It is by no means the only method that could have been applied to it, but the following reasons made it more attractive than others:

1. The amount of information required from the DM is limited and easier to provide. For example, there is no need to give relative importance of the criteria.
2. The method has been applied on real-life cases (Paris suburb expansion plans).
3. The method will not draw strong conclusions if the available data does not permit to do so. It also provides a solution where other methods cannot due to insufficient data.
4. The property assumptions (existence of function, additivity, etc.) required for other methods such as the multi attribute utility function, are not necessary in the ELECTRE IV method. The result of this fact is that the method will not necessarily be able to provide a complete order of the alternatives.

As mentioned in reason no. 1, this method does not require the DM to express his priority in terms of the criteria. Instead, he or she should indicate what his/her thresholds are with respect to indifference and preference. An indifference threshold for a particular criterion is the maximum change in the attribute of that criterion for which the DM is indifferent. In more common language, it is the largest change that goes unnoticed. A preference threshold is the smallest difference between two attributes of one criterion for which the DM can make a preference. These thresholds can be either fixed or dependent on the value of the attribute for a particular criterion. The indifference threshold can also be regarded as a way to take into account the inaccuracy of the pay-off values. The main steps are of the method are as follows:

Step 1: setting the thresholds

For an action a being *strictly preferred* to an action a' with respect to criterion i, the following condition should be fulfilled. $g_i(a)$ is the level of satisfaction or the score of alternative a with respect to criterion i

$$g_i(a) \geq g_i(a') + p_i(g_i(a'))$$

where p_i is the preference threshold given as a function of $g_i(a')$.

An action a would be called *weakly preferred* to an action a' with respect to criterion g_i, if the following condition is satisfied.

$$g_i(a') + p_i(g_i(a')) \geq g_i(a) \geq g_i(a') + q_i(g_i(a'))$$

where q_i is the indifference threshold depending on the value $g_i(a')$.

This concept of thresholds is illustrated in Figure 6-1. The value u represents the difference between the scores of two alternatives for one criterion.

$$u = g_i(a') - g_i(a) \qquad (u \geq 0)$$

When u is smaller than q_j, a and a' are said to be *indifferent* to each other for criterion j (1). For u between q_j and p_j, a' is declared *weakly preferred* to a (2), while when u is larger than p_j (3), a' is strictly preferred to a. The veto threshold (v_j) is used in step 3 to distinguish between strong and weak outranking relations.

The same reasoning is applicable when u is defined as

$$u = g_i(a) - g_i(a') \qquad (u \geq 0)$$

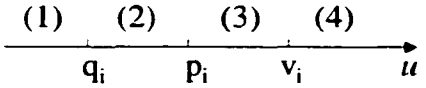

Figure 6-1. Preference and indifference thresholds.

Step 2 – checking the strong and weak preferences

With the thresholds provided in the first step, the alternatives should be compared with each other for their scores for the different criteria. It is evaluated for how many criteria one alternative is preferred to another one. And this is repeated for three levels of preferences: weak, strong and veto. The veto preference has usually a threshold that is two times the strong preference threshold.

Step 3: defining the outranking relations

Now, two outranking relations are introduced, based on the previous preference concepts.

$aS_F a'$ a *strongly* outranks a' if no criterion exist for which a' is strictly preferred to a and the number of criteria for which a' is weakly preferred to a is at most equal to the number of criteria for which a is preferred (weakly or strongly) to a'.

$aS_f a'$ a *weakly* outranks a' if no criterion exists for which a' is strictly preferred to a, but the second condition for the strong outranking is not fulfilled; or if there exists a unique criterion for which a' is strictly preferred to a, under the condition that the difference in favor of a' is not larger than the veto threshold and that a is strictly preferred for at least half of the criteria.

Step 4: distillation

In this step it is verified for each action how many other actions it strongly outranks, and by how many other actions it is strongly outranked. The difference between both is called the strong qualification. A weak qualification is obtained in a similar fashion.

Two rankings are obtained. For the first one, descending distillation, the action with the largest strong qualification is selected and will receive the rank number 1. The qualifications of the remaining alternatives are recalculated, this time without the selected alternative. The alternative that has the highest qualification is selected this time for the second spot. This is continued until all alternatives have been selected. In case of a tie in the strong qualifications, the weak qualifications are used to break the tie.

A second ranking, ascending distillation, is obtained by using the same procedure, but now the alternative with the lowest strong qualification is selected for the lowest rank. The qualifications are recalculated again, and again the alternative with the lowest is selected. This is repeated until all options are selected.

Step 5: final ranking

A final ranking is obtained by combining the two rankings obtained in the previous step. This ranking can be represented by a graph. An arrow points from a node representing the preferred action to the node of the outranked action (e.g., a to b, Figure 6-2). Two equivalent actions are represented by the same node (d and e). Actions that are incomparable are not linked with an arrow, but are located at the same ranking level (b and c). This means that, when comparing *b* and *c*, there are not only strong reasons in favor of *b* and against *c*, but also strong reasons in favor of c and against *b*. Both *b* and *c* are outranking *d* and *e*, but are worse than *a*.

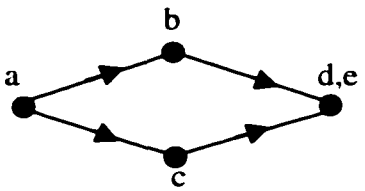

Figure 6-2. Example of final order with ELECTRE IV.

6.9 Results obtained with ELECTRE IV

The ELECTRE IV method will now be applied to the decision problem presented in section 6.1.

Step 1 – defining the thresholds.

Lets assume that the Decision Maker chooses the following thresholds. The veto thresholds are taken as the double of the preference threshold. The values in Table 6-8 are percentages of the score of an alternative for a particular criterion.

Table 6-8. Threshold values.

%	Indifference	Preference	Veto
Profits	30	50	100
Risk	5	20	40
Variance	15	40	80

Step 2 – checking the strong and weak preferences

The following tables indicate for how many criteria the action at the left of a row is preferred to the action at the top of the column. Table 6-9 refers to the weak preference, Table 6-10 to the strong preference while Table 6-11 shows the result with respect to the veto preference.

Table 6-9. Weak preferences.

		Weak preference		
	Action 1	***Action 2***	***Action 3***	***Action 4***
Action 1		0	0	1
Action 2	0		0	0
Action 3	0	0		0
Action 4	0	0	0	

Table 6-10. Strong preferences.

		Strict Preference		
	Action 1	***Action 2***	***Action 3***	***Action 4***
Action 1		0	1	0
Action 2	2		1	2
Action 3	2	0		2
Action 4	0	0	1	

Table 6-11 - Veto preferences

		Veto Preference		
	Action 1	***Action 2***	***Action 3***	***Action 4***
Action 1		0	0	0
Action 2	1		0	1
Action 3	1	0		1
Action 4	0	0	1	

Step 3 – outranking relations

In this step for each pair of actions, it is decided whether one action strongly or weakly outranks the other or not at all. It can also happen that two actions outrank each other. Consequently, the outranking hypothesis should be checked in both directions.

An 'F' indicates that the action at left outranks strongly the action at the top of the column. On the other hand a lowercase 'f' points towards a *weak* outranking relation. The results are shown in Table 6-12. It can be seen here that action 1 strongly outranks action 4, but on the other hand action 4 weakly outranks action 1.

Table 6-12 - Weak and strong outranking relations

		Outranking		
	Action 1	***Action 2***	***Action 3***	***Action 4***
Action 1		0	0	F
Action 2	F		F	F
Action 3	f	f		0
Action 4	f	0	0	

Step 4 – distillation procedure

Table 6-12 is now used to extract two rankings, one using descending distillation, and one using ascending distillation. In Table 6-13 the numbers below each action refer to the actions that are strongly outranked by the action in the first row. In Table 6-14 the weakly outranked actions are listed.

Table 6-13 - Strong outranking relations

Action 1	*Action 2*	*Action 3*	*Action 4*
4	1,3,4		

Table 6-14 - Weak outranking relations

Action 1	*Action 2*	*Action 3*	*Action 4*
		1,2	1

The qualifications can now be obtained for each action. The strong qualification for an action is the difference between the number of actions that it strongly outranks with the number of actions it is strongly outranked by. A weak qualification is similarly obtained in a similar fashion. The results are displayed in Table 6-15 and in Table 6-16.

Table 6-15. Strong qualifications.

Action 1	*Action 2*	*Action 3*	*Action 4*
0	3	-1	-2

Table 6-16. Weak qualifications.

Action 1	*Action 2*	*Action 3*	*Action 4*
-2	-1	0	0

The descending distillation works as follows: The action with the highest strong qualification is chosen. In this case it is action 2. In the case of an ex-aequo, the weak qualifications are used to untie. When even the weak qualifications are the same, the 2 actions are selected and considered equivalent for that ranking procedure. Action 2 is ranked first and consequently removed from Table 6-13 and Table 6-14; the new qualifications are calculated. The distillation procedure is continued until all actions are ranked. The ranking obtained this way is:

$$2 \rightarrow 1 \rightarrow 3,4$$

Action 3 and 4 are equivalent in this ranking. The ascending distillation works in the same way but starts by selecting the action with the lowest strong qualification, which is action 4. It is ranked last and then removed from the two tables, etc. The ranking obtained like this gives:

$$2 \rightarrow 3 \rightarrow 1 \rightarrow 4$$

Step 5 - graphical final order

From the two rankings obtained in the previous step, a final order can be extracted. We see that in both rankings, action 2 is on the first spot. So this will be the action with the first priority. Next, we see that 1 and 3 have the spots 2 and 3 respectively in the first ranking, and spots 3 and 2 in the second ranking. Those two actions are declared incomparable. Finally, we see that both actions 1 and 3 are ranked higher than action 4 in any of the rankings. Action 4 will have the last priority. Graphically, the relations can be visualized as shown in figure 6-3.

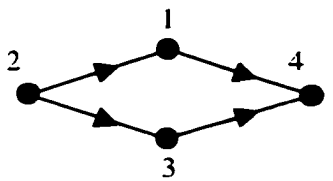

Figure 6-3. Final ranking.

From this result, the DM knows that there are strong reasons that favor action 2 over all the others, while no strong reasons against this decision exist. Due to the fact that the method allows incomparability[7], it does not recommend – in this case – a second-best solution, as Action 1 and 3 are incomparable; should a choice between 1 an 3 be necessary, the DM would have to analyze the alternatives further to make a final decision. However, it should be pointed out that, if a complete order (without ties) of the alternatives is desired, other variants of the ELECTRE IV method could be employed, as well as other outranking methods [91].

[7] This characteristic is also called non-prescriptiveness.

6.10 Sensitivity analysis

The results presented above only refer to one set of thresholds. It is recommended to verify how solid the suggested results are for slight changes in the data, in particular, in the data provided by the DM. When changing the thresholds, one of the major advantages of the ELECTRE IV method becomes obvious: the influence of the thresholds, i.e., the input of the DM, on the final result is only partial.

This is as opposed to the multi-criteria method with scaling coefficients, where almost any alternative can come out on top depending exclusively on the value of the weights. This leads to a much greater responsibility for the DM. With the ELECTRE IV method, the final solution is determined for a great deal by the values of the attributes and only partially by the information given by the DM. In the following the results are shown of the application of the ELECTRE IV method to several different sets of thresholds (Table 6-17 to Table 6-22).

Table 6-17. Example 1

	Q	*P*	*V*
Profits	0	0.4	0.8
Risk	0	0.2	0.4
St. Deviation	0	0.4	0.8

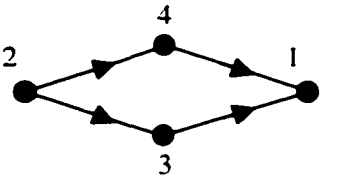

Figure 6-4. Graphical final order of example 1

Table 6-18. Example 2

	Q	*P*	*V*
Profits	0	0.05	0.1
Risk	0	0.05	0.1
St. Deviation	0	0.05	0.1

Figure 6-5. Graphical final order of example 2

Table 6-19. Example 3

	Q	*P*	*V*
Profits	0.4	0.5	1.0
Risk	0.4	0.5	1.0
St. Deviation	0.4	0.5	1.0

Figure 6-6. Graphical final order of example 3

Table 6-20. Example 4

	Q	*P*	*V*
Profits	0.4	0.4	0.8
Risk	0.2	0.2	0.4
St. Deviation	0.4	0.4	0.8

Figure 6-7. Graphical final order of example 4

Table 6-21. Example 5

	Q	*P*	*V*
Profits	0.2	0.4	0.8
Risk	0	0.05	0.1
St. Deviation	0.2	0.4	0.8

Figure 6-8. Graphical final order of example 5

Table 6-22. Example 6

	Q	*P*	*V*
Profits	0.2	0.4	0.8
Risk	0.2	0.4	0.8
St. Deviation	0	0.05	0.1

Figure 6-9. Graphical final order of example 6

Table 6-23. Example 7

	Q	*P*	*V*
Profits	0	0.05	0.1
Risk	0.2	0.4	0.8
St. Deviation	0.2	0.4	0.8

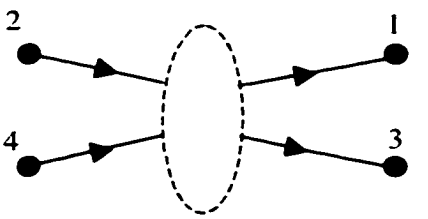

Figure 6-10. Graphical final order of example 7

As the results suggest, when the different thresholds are changed over a large range, alternative 2 always remains among the favorites. The influence of the thresholds is more perceptible in the ranks of less attractive alternatives.

Generally speaking, the ranking of an alternative will improve, as the threshold for the criterion for which it performs best, gets tighter. An example of this is alternative 4, which has the highest profits. When making the thresholds for the profits tighter, alternative 4 will rise in the ranking.

6.11 Summary of the chapter

This chapter describes how risk can be used in decision making for power system operation. First, a decision making case is presented where a plant operator has to choose among several operating alternatives for the next hour. Different, single criterion decision-making strategies are applied to this problem and their weaknesses are exposed. It is explained why variance should also be included in the decision-making problem.

Next, it is argued that multiple criteria decision-making (MCDM) techniques are more suitable for this kind of problems. An overview of the existing MCDM methods is presented, and one of them is applied to the stated problem and the results are discussed.

7. CONCLUSIONS AND FURTHER WORK

7.1 Contribution of this work

The main topic of the work presented in this dissertation is the quantification of transient instability risk. The complete methodology and some important related issues have been addressed. The following list summarizes the most significant contributions presented in this dissertation.

Risk of transient instability assessment method

Elaboration of detailed probability expressions

Expressions for computing the risk of transient instability are evolved to include probabilistic models for the uncertainties regarding the fault occurrence, location of the fault on the line, the type fault, the fault clearing time, and the pre-fault load levels.

Influencing factors for transient instability risk

The influence on the maximum generation limit of various factors including the fault and operating parameters are evaluated, and it was found that the errors on the fault clearing time does considerably affect this limit: situations are identified that are deterministically secure, but have a risk value greater than zero. It is also shown that other parameters, such as the terminal voltage level and local load, have a smaller but significant influence on the risk.

Evaluation of the impact of transient instability

The different components of the impact resulting from a transient instability event are identified and modeled.

Use of hybrid transient stability assessment method

The hybrid method allows termination of the transient stability simulation as soon as the (in)stability has been detected and evaluates the degree of (in)stability. This method is integrated in the risk calculation algorithm.

Development of a software package

A software package was developed to implement the risk of transient instability calculation methodology.

Fast risk assessment

Several techniques are suggested to improve the speed of the risk calculation and to make the method more practical. In particular, the use of artificial neural networks for risk-based nomogram plotting is illustrated.

Risk-based decision making for power system operation

A method is provided to approach the problem of decision-making in power system operation as a multi-criteria decision making problem to which multi-criteria decision making tools can be applied, with the following three criteria: maximizing expected profits, minimizing risk associated with each action, and minimizing the variance of the impact of each action.

7.2 Further work

It would also be worthwhile to evaluate the impact of transient instability in terms of the effect on the risk of cascading events and islanding of the system.

The evaluation of the risk has already been developed for most security problems. However, it would be of great interest to also develop a method to calculate the risk of oscillatory instability. Due to the interest that many utilities have in the problem, the risk method to quantify risk of voltage dip violation should be developed further; the method should be implemented and solutions should be found to reduce its computation time.

It would also be significant to combine all risks indices into one composite risk index, as is suggested in [99], where this composite risk could be used to plot contours of equal risk in risk-based nomograms and to incorporated in a decision support tool based on the concepts developed in this dissertation. At the same time, it would also be necessary to determine *composite variance*.

In this work, it was assumed the different options available to the decision-maker were known. It is therefore necessary to develop a procedure to define a set of credible and reasonable corrective actions for the decision-maker to choose from in using the decision aid tool.

7.3 Conclusions

The motivation behind this work is that it is essential for the operators to know more than just the deterministic operating limits for their system, and in the case of transient instability, the limits for the generators. As mentioned earlier, transient instability risk is a part of risk based security assessment, which offers a new way of dealing with power system security by looking at the probability of the insecurity events and the consequences of these events. Transient instability is a particular type of insecurity that is complicated to assess, requiring special attention to make the risk calculation not too time-consuming. It also allows identification of the risk associated with deterministically secure situations.

The results show that system operation could be improved by taking into account the risk associated with an operating point. Besides revealing operating areas within the deterministically secure region with low or no risk, the method also measures the risk outside the secure region. This opens possibilities for an operator who is not risk averse and would be prepared to operate outside the secure area if, according to the decision maker, the

expected benefits exceeds the risk. This capability is of great interest in the competitive electric power industry.

REFERENCES

[1] NERC, Planning Standards, draft June 1997.

[2] Western Systems Coordinating Council Reliability Criteria, March 1997.

[3] Silverstein B., Porter D., "Contingency Ranking for Bulk System Reliability Criteria," IEEE Trans. Pwr. Sys., Vol. 7, No. 3, Aug. 1992, pp. 956-964.

[4] Alvarado F., Hu Y., Ray D., Stevenson R., Cashman E., "Engineering Foundations for the Determination of Security Costs," IEEE Trans. Pwr. Sys., Vol. 6, No. 3, Aug. 1991, pp. 1175-1182.

[5] Leite da Silva, A., Endrenyi J., Wang L., "Integrated Treatment of Adequacy and Security in Bulk Power System Reliability Evaluations," IEEE Trans. Pwr. Sys., Vol. 8, No. 1, Feb 1993, pp. 275-285.

[6] Counan C., Trotignon M., Corradi E., Stubbe M., Deuse J., "Major Incidents on the French Electric System: Potentiality and Curative Measures Studies," IEEE Trans. Pwr. Sys., Vol. 8, No. 3, Aug. 1993, pp. 879-886.

[7] Aboreshaid S., Billinton R., "A Framework for Incorporating Voltage and Transient Stability Considerations in Well-Being Evaluation of Composite power systems," in *Proceedings of the Power Engineering Society Summer Meeting*, Edmonton AB., 1999, July 99, Vol. 1, pp. 219–224.

[8] Porretta B., Kiguel D., Hamoud G., Neudorf E., "A Comprehensive Approach for Adequacy and Security Evaluation of Bulk Power Systems," IEEE Trans. Pwr. Sys., Vol. 6, No. 2, May 1991, pp. 433-441.

[9] EPRI final report WO8604-01, "Risk-based Security Assessment," December 1998.

[10] Wan H., McCalley J., Vittal V., "Increasing Thermal Rating by Risk Analysis", IEEE Trans. Pwr. Sys., Vol. 14, No. 3, August 1991, pp. 815–828.

[11] Wan H., McCalley J., Vittal V., "Risk Based Voltage Security Assessment", submitted for review to the IEEE Transactions in Power Systems.

[12] Dai Y., *Framework for Power System Annual Risk Assessment*. Ph.D. dissertation, Iowa State University, 1999.

[13] Fu W., *Risk Assessment and Optimization for Electric Power Systems*. Ph.D. dissertation, Iowa State University, 2000.

[14] Kundur P., *Power Stability and Control*. Power System Engineering Series, McGraw Hill, New York, 1994.

[15] Arrillaga J., *Computer Modeling of Electrical Power Systems*. Wiley & Sons, New York, 1983.

[16] Stagg, G.W., El-Abiad, A.H., *Computer Methods in Power System Analysis*. McGraw Hill, New York, 1968.

[17] Boyce, W. E., DiPrima, R. C., *Elementary Differential Equations and Boundary Value Problems*. Wiley and Sons, New York, 1977.

[18] Fouad A. A., Vittal V., *Power System Transient Stability Analysis Using The Transient Energy Function Method*. Prentice Hall, Englewood Cliffs, NJ, 1992.

[19] Pai, M.A., *Energy Function Analysis for Power System Stability*. Kluwer Academic Publisher Boston 1989.

[20] Kakimoto N., Ohsawa Y., and Hayashi M., "Transient Stability Analysis of Electric Power System Via Lure' Type Lyapunov Functions, Parts I & II," Transactions of IEE of Japan, Vol. 98, No. 516, May/June 1978.

[21] Athay T., Sherkat V.R., Podmore R., Virmani S., and Puech C., "Transient Energy Analysis," Final report of U.S. Department of Energy Contract No. EX-76-C01-2076, Prepared by systems Control Inc., June 1979.

[22] Chiang H.D., Wu F.F, and Varaiya P.P., "Foundations of the potential energy boundary surface method for power systems," IEEE Transactions of CAS, Vol. 35, June 1988, pp. 712-728.

[23] Xue Y.; Van Cutsem Th.; Ribbens-Pavella M., "A simple direct method for fast transient stability assessment of large power systems," IEEE Trans. Pwr. Sys., Vol. 3, No. 2, May 1988, pp. 400-412.

[24] Xue Y.; Van Cutsem Th.; Ribbens-Pavella M., "Extended Equal Area Criterion Justifications, Generalizations, Applications," IEEE Trans. Pwr Sys., Vol. 4, No. 1, Feb 1989 pp. 44-52.

[25] Fouad A.A., Kruempel K.C., Vittal V., Ghafurian, A., Nodehi K., and Mitache J.V., "Transient Stability Program Output Analysis," IEEE Trans. Pwr Sys., Vol. 1, No 1., Feb 1986 pp. 2-9.

[26] Maria G., Tang, C.K., Kim J., "Hybrid Transient Stability Analysis," IEEE Trans. Pwr. Sys., Vol. 5, No. 2, May 1990, pp. 384-393.

[27] Tang C.K., Graham C.E., El-Kady M., Alden R.T.H., "Transient Stability Index from Conventional Time Domain Simulation," IEEE Trans. Pwr. Sys., Vol. 9, No. 3. Aug.1994, pp. 1524-30.

[28] Chang H-C., Chen H-C., "A Mixed Direct Method for Transient Stability Assessment," Journal of the Chinese Institute of Engineers. Vol. 16, No. 3, 1993, pp. 355-366.

[29] Zhang Y.L., Wehenkel L., Pavella M.,"SIME: a Hybrid Approach to Fast Transient Stability Assessment and Contingency Selection," Journal of EPES, Vol. 19, No. 3, 1997, pp. 195-208.

[30] Ejebe G.C., Jing C., Vittal V., Waight J.G., Pieper G., Jamshidian F., Sobajic D., Hirsch P., "On-line Dynamic Security Assessment: Transient Energy Based Screening and Monitoring for Stability Limits", paper presented at the IEEE Summer Meeting in Berlin, Germany, 1997.

[31] Burchett R.C., Heydt G.T., "Probabilistic Methods for Power System Dydnamic Stability Studies," IEEE Trans. on Pwr. App. And Sys., Vol. PAS-97, No. 13, May/June 1978, pp. 695-702.

[32] Billinton R., Kuruganty P., "A Probabilistic Index for Transient Stability," IEEE Trans. on Pwr. App. And Sys.,. Vol. PAS-99, No. 1, Jan/Feb 1980, pp. 195-206.

[33] Kuruganty P., Billinton R., "A Probabilistic Assessment of Transient Stability," International Journal of Electric Power and Energy Systems, Vol. 2, No. 2, 1980, p 115-119.

[34] Billinton R., Kuruganty P., "Probabilistic Evaluation of Transient Stability in Practical Multimachine Power Systems," IEEE Trans. on Pwr. App. And Sys., Vol. PAS-100, No. 7, July 1981, pp. 3634-3641

[35] Kuruganty P., Billinton R., "Protection System Modeling in a Probabilistic Assessment of Fault Clearing Time," IEEE Trans. on Pwr. App. And Sys., Vol. PAS-100, No. 5, May 1981, pp 2164-2170.

[36] Anderson P., Bose A., "A Probabilistic Approach to Power System Analysis," IEEE Trans. on Pwr. App. And Sys., Vol. PAS-102, No. 8, August 1983, pp. 2430-2439.

[37] Bose A., Anderson P., Timko K., Villaseca F., "A Probabilistic Approach to Stability Analysis," EPRI report EL-2797, 1983.

[38] Timko K., Bose A., Anderson P., "Monte-Carlo Simulation of Power Systems Stability," in *Proceedings of the Power Industry Computer Applications Conference* (PICA), 1983.

[39] Wu F., Tsai Y., Yu Y., "Probabilistic Steady-State and Dynamic Security Assessment," IEEE Trans. Pwr. Sys., Vol. 3, No. 1, Feb. 1988, pp.1-9.

[40] Leite da Silva, A., Endrenyi J., Wang L., "Integrated Treatment of Adequacy and Security in Bulk Power System Reliability Evaluations," IEEE Trans. Pwr. Sys., Vol. 8, No. 1, Feb 1993, pp. 275 -285.

[41] Hsu Y-Y., Chang C.-L., "Probabilistic Transient Stability Studies using the Conditional Probability Approach," IEEE Trans. Pwr. Sys., Vol. 3, No. 4, Nov. 1988, pp. 1565-1572.

[42] Chiodo E., Lauria D., "Transient Stability Evaluation of Multimachine Power Systems: a Probabilistic Approach Based Upon Extended Equal Area Criterion," IEE Proc. Gener. Transm., Vol. 141, No. 6, 1994, pp. 545 -553.

[43] Momoh J.A., Elfayoumy M., Mittelstadt W., Makarov Y. V., "Probabilistic Angle Stability Index," in *Proceedings of the Power Engineering Society Summer Meeting*, Edmonton AB., 1999, July 99, Vol. I, pp. 212 –218.

[44] Dodu J., Merlin A., "New Probabilistic Approach Taking into Account Reliability and Operation Security in EHV Power System Planning at EDF," IEEE Trans. Pwr. Sys., Vol. 1, No. 3, Aug. 1986.

[45] Irizarry-Rivera A.A., *Risk-Based Operating Limits For Dynamic Security Constrained Electric Power Systems.* PhD-dissertation, Iowa State University, 1996.

[46] McCalley J. D., Fouad, A. A., Agrawal B. L., Farmer R. G., Vittal V., Irizarry-Rivera A., "A Risk-Based Security Index for Determining Operating Limits in Stability-Limited Electric Power Systems," IEEE Trans. Pwr. Sys. Vol. 12, No. 3, Aug. 1997, pp. 1210-1219.

[47] Sreedhara R. *Transient voltage dip analysis using the Transient Energy Function method.* Master of Science thesis, Iowa State University, 1999.

[48] Fouad, A. A., Sreedhara, R., "Transient voltage dip analysis using the transient energy function method," in *Proceedings of the Annual North American Power Symposium*, 1990.

[49] Bollen M., *Understanding Power Quality Problems.* IEEE press series on Power Engineering, New York, 1999.

[50] Debs A., "Voltage dip at maximum angular swing in the context of direct Stability analysis," IEEE Trans. Pwr. Sys., Vol. 5, No. 4, Nov. 1990, pp 1497-1502.

[51] Debs, A., Dominguez, F., "Sensitivity analysis of voltage dip computations using the TEF methods," in *Proceedings of the IEEE Conference on Decision and Control* Vol. 6 Dec 5-7 1990, pp 3031-3032.

[52] Treinen, R., Vittal V., Fouad A.A, "Application of a Modal-Based Transient Energy Function to a Large-Scale Stressed Power System: Assessment of Transient Stability and

Transient Voltage Dip," International Journal of Electrical Power and Energy System Vol. 15, No 2, April 1993, pp. 117-125.

[53] Djukanovic M., Sobajic D., Pao Y-H., "Neural-net Based Calculation of Voltage Dips at Maximum Angular Swing in Direct Transient Stability Analysis," International Journal of Electrical Power and Energy Systems, Vol. 14, No.5, October 1992, pp.341-350.

[54] "The IEEE Reliability Test System - 1996," a report prepared by the Reliability Test System Task Force of the Application of Probability Methods Subcommittee, IEEE Trans. Pwr. Sys., Vol. 14, No. 3, August 1999, pp. 1010 -1020.

[55] "Analytical Methods for Contingency Selection and Ranking for Dynamic Security Analysis," EPRI Final report TR-104352, project 3103-03, Sept. 1994.

[56] Haykin S., *Neural Network, A comprehensive foundation.* McMillan Publishing, New York, NY, 1994.

[57] El-Sharkawa M. and D. Niebur, editors, "Artificial Neural Networks with applications to Power Systems," IEEE PES special publication 96 TP 112-0, 1996.

[58] Pang C.K., Prabhakara F.S., El-Abiad A, Koivo A.J. "Security Evaluation in Power Systems Using Pattern Recognition," IEEE Trans. Power Apparatus and Systems Vol. PAS-93, No. 3, May-Jun 1974 p 969-976.

[59] Sobajic D., Pao Y-H., "Artificial Neural-Net Based Dynamic Security Assessment for Electric Power," IEEE Trans. Pwr. Syst. Vol. 4, No.1, Feb. 1989, pp. 220-226.

[60] Mansour Y., "Dynamic Security Contingency Screening and Ranking Using Neural Networks," IEEE Trans. Neural Networks. Vol. 8, July 1997 p. 942-50.

[61] Miranda V., Fidalgo J.N., Lopes, J.A.P., and Almeida L.B "Real Time Preventive Actions for Transient Stability Enhancement with a Hybrid Neural Network-Optimization," IEEE Trans. Pwr. Syst. Vol. 10, No.1, May 1995, pp. 1029-1035.

[62] Fidalgo J.N., Peças Lopes J.A., Miranda, V., "Neural Networks Applied to Preventive Control Measures for the Dynamic Security of Isolated Power Systems with Renewables," IEEE Trans. Pwr. Sys., Vol. 11, No. 4, Aug. 1996, pp. 1811-1816.

[63] Kumar A.B.R., Ipakchi A., Brandwajn V., El-Sharkawi M., Cauley G. "Neural Network for Dynamic Security Assessment of Large-Scale Power Systems: requirements overview", in *Proceedings of the 1st International forum on applications of Neural Network to Power Systems*, Seattle, 1991.

[64] Christie R.D., Talukdar S.N., and Nixon J.C., "CQR: A Hybrid Expert System for Security Assessment," IEEE Trans. Pwr. Syst. Vol. 5, No.4, Nov. 1990, pp. 1503-1509.

[65] Wehenkel L., Pavella M., Euxibie E., Heilbronn B.,"Decision Tree Based Transient Stability Method – A case study," IEEE Trans. Pwr. Sys., Vol. 9, No. 1, Febr. 1994, pp. 459–469.

[66] Song Y., Zeng Q., and Han Y., "Framework of Fast Stability Assessment of Power System by Neural Network-based Pattern Recognition," Advances in Power System Control, Operation and Management, 1991. APSCOM-91, Vol.2, pp. 578-581.

[67] Peças Lopes, J.A., Vasconcelos M.H., "On-line Dynamic Security Assessment Based on Kernel Regression Trees," in *Proceedings of the Power Engineering Society Summer Meeting*, Singapore, Jan. 2000.

[68] Van Acker V., McCalley J.D., Vittal V., Mitchell M., "Risk Based Transient Stability Assessment using Neural Networks", in *Proceedings of the 30th North American Power Symposium*, Cleveland, Ohio, 1998, pp. 328-335.

[69] Kumamoto H., Henley E.J., *Probabilistic Risk Assessment and Management for Engineers and Scientist*. IEEE press, 2nd Edition, New York, 1996.

[70] Van Acker V., Wang S., McCalley J.D., Zhou G., Mitchell M.,"Data Generation Using Automated Security Assessment for Neural Network Training," in *Proceedings of the 29th North American Power Symposium*, Laramie, WY,1997.

[71] Zhou G., *Power system security boundary visualization using intelligent*. Ph.D. Dissertation Iowa State University, 1998

[72] Vafaie H. and Jong K.D., "Genetic Algorithms as a Tool for Feature Selection in Machine Learning," Fourth International Conference on Tools with Artificial Intellligence TAI'92, Arlington, VA, Nov., 1992, pp. 200-203.

[73] Goldberg, D.E., *Genetic Algorithms in Search Optimization and Machine Learning*. Addison-Wesley, Reading, MA.

[74] EPRI final report WO8604-01, "Risk-based Security Assessment," December 1998.

[75] Van Acker V., McCalley J.D., Vittal V., Peças Lopes J. A., "Risk-based Transient Stability Assessment," in *Proceedings of the Budapest Powertech Conference*, Budapest, Hungary, 1999.

[76] Anders G.J., *Probabilistic concepts in electric power systems*. John Wiley & Sons, New York, 1990.

[77] Chankong V., Haimes Y.Y., *Multi-objective Decision Making – Theory and Methodology*. North Holland, New York, 1983.

[78] Lindley D.V., *Making Decisions*. Wiley &Sons, London, UK, 2nd Edition, 1985.

[79] Kmietowicz, Z.W., Pearman A.D., *Decision Theory and Incomplete Knowledge*. Gower, Hampshire, UK, 1981.

[80] Churchman C.W., Ackoff R., Arnoff E., *Introduction to Operation Research*. Wiley & Sons, New York, NY, 1957.

[81] Raiffa H., *Decision Analysis*. Addison-Wesley, Reading, MA, 1968

[82] Keeney R.L., Raiffa H., *Decisions with Multiple Objectives – Preferences and value trade-offs*. Wiley & Sons, New York, NY, 1976.

[83] Saaty T.L., *Analytical Hierarchy Process*. McGraw Hill, New York, NY, 1980.

[84] Roy B., "Classement et Choix en Présence de Points de Vue Multiples (la méthode ELECTRE)," Revue Française d'Informatique et de Recherche Opérationelle Vol. 8, 1968, pp 57-75.

[85] Roy, B., Bertier P., "La Méthode ELECTRE II," Working paper 142, SEMA, 1971.

[86] Roy.B., Bertier P., "La Méthode ELECTRE II, une application au media-planning." OR 72, M. Ross editor, North Holland, New York, 1973, pp. 291-302.

[87] Roy B., "ELECTRE III: Algorithme de Classement Basé sur une Représentation Floue des Préférences En Présence de Critères Multiples," Cahiers de CERO Vol. 20, No. 1, pp. 3-24.

[88] Hugonnard J., Roy B., "Ranking of Suburban Line Extension Projects for the Paris Metro System by a Multi-Criteria Method," Transportation Research 16A, 1982, pp. 301-312.

[89] Gal T., et al (ed), *Multicriteria Decision Making*. Kluwer, London, 1999.

[90] Roy B., Bouyssou D., "Aide Multicritère à la Décision: Méthodes et Cas." Economica, Paris, 1993.

[91] Vincke Ph., "Outranking Approach," in Multicriteria Decision Making, Gal. T. et al. (ed.), Kluwer, London, 1999.

[92] Brans J.P., Vincke, Ph., "A Preference Ranking Organization Method." Management Science Vol. 31, No. 6, 1985, pp. 647-656.

[93] Charnes A., Cooper W.W., *Management Models and Industrial Applications of Linear Programming*, Wiley, New York, 1961.

[94] Romero C., "A Survey of Generalized Goal Programming (1970-1982)," European Journal of Operational Research, Vol. 25, 1986, pp. 183-191.

[95] Stewart T.J., "A Critical Survey on the Status of Multiple Criteria Decision Making-Theory and Practice," OMEGA, Intl. Journal of Management Science, Vol. 20, No. 5/6, 1992, pp. 569-586.

[96] Hobbs, B.F., Chankong, V., Hamadeh, W., Stakiv E.Z. "Does the Choice of Multi-criteria Method Matter? An Experiment in Water Resources Planning," Water Resources Research, Vol. 28 No. 7, July 1992, pp. 1767-1779.

[97] Zanakis S.H., Solomon A., Wishart N., Dublish S., "Multi-attribute Decision Making: a Simulation Comparison of Select Methods," European Journal of Operational Research, Vol. 107, 1998, pp. 507-529.

[98] Vincke, Ph., *Multicriteria Decision-aid.* translated from French, Wiley & Sons, New York, NY, 1992.

[99] Wan H., *Risk-based Security Assessment for Operating Electric Power Systems.* PhD-dissertation, Iowa State University, 1999.

ACKNOWLEDGEMENTS

Above all, I must thank my major professor Dr. James D. McCalley for the guidance of my research and for giving me courage and confidence during my stay at Iowa State University. It was a real pleasure to work with him.

I also would like to thank Dr. João A. Peças Lopes, whose enthusiasm convinced me to choose for power systems, for taking time twice to come all the way from Porto, Portugal to attend both Ph. D. examinations. I am also very grateful to Drs. V. Vittal, V. Honavar, R. Barton, and S. Vardeman, for generously providing suggestions and assistance in the completion of this work. I would also like to thank Dr. Nuno Fidalgo for his valuable help in training the neural networks used in this work, and Matthew Mitchell for the long hours we spent together trying to get the dataset generation software working.

It has been a wonderful experience to be part of such a diverse and enthusiastic group of power system graduate students. In particular I would like to mention Nagaraj, for his impressive knowledge and spiritual guidance, Chuck, for making work at ISU more bearable and even fun, and to Songzhe, Madhura, Sunitha, Xuezhen, Huazhong, Mona, Youjie, Xuechun, Weihui, Chuanjiang, Huang Jiang, and many others that passed by Coover during these four years: to all of you I would like to say, thank you.

A very special thanks for my best friend in life, Dadi, who shared with me the failures, anxieties, stress and frustrations and has been my life-support during these years, and for my father who, despite the distance, never spares any effort to encourage me and to help me through the difficult moments.

Finally, I would like to thank the Foundation of Science and Technology, Portugal - PRAXIS XXI Program BD/9298/96 for the financial support granted.